State of Delaware
DELAWARE GEOLOGICAL SURVEY
John H. Talley, State Geologist

REPORT OF INVESTIGATIONS NO. 65

WELLHEAD PROTECTION AREA DELINEATIONS FOR THE LEWES-REHOBOTH BEACH AREA, DELAWARE

by

A. Scott Andres

Cheryl A. Duffy

Evan M. Costas

University of Delaware
Newark, Delaware

2003

CONTENTS

	Page
ABSTRACT	1
INTRODUCTION	1
Purpose and Scope	1
Previous Digital Flow Modeling Studies	1
Acknowledgments	1
GENERAL HYDROGEOLOGY	2
Lithostratigraphic Units and their Hydrologic Functions	3
Aquifer Tests	5
Ground-Water Levels	6
METHODS	6
Model Implementation	6
Hydraulic Conductivity	7
Boundary Conditions	8
Model Calibration	11
Adjustments to Calibration Dataset	13
Particle Tracking and Wellhead Protection Area Delineation	13
Sensitivity Analysis	14
RESULTS AND DISCUSSION	14
Calibration to Pre-Pumping Conditions	14
Pumping and Drawdown	15
Sensitivity Analysis	17
WHPA Recommendations	18
CONCLUSIONS	20
REFERENCES CITED	22
APPPENDIX	
Conversion factors	23

ILLUSTRATIONS

		Page
Figure 1.	Location map of the study area and wellfields.	2
2.	Generalized geologic map of study area.	3
3.	Cross-sectional hydrogeologic model.	4
4.	Map of model grid and study area.	6
5.	Cross-sectional view of model grid along row 113.	7
6.	Map showing spatial pattern of K (m/s) for layer 1.	8
7.	Map showing spatial pattern of K (m/s) for layer 2.	8
8.	Map showing spatial pattern of K (m/s) for layers 3-4.	9
9.	Map showing spatial pattern of K (m/s) for layer 5.	9
10.	Map showing spatial pattern of K (m/s) for layer 6.	10
11.	Map of model boundary cells for layer 1.	10
12.	Map of model boundary cells for layers 2-6.	11
13.	Map showing spatial pattern of recharge for uppermost active layer.	11
14.	Map showing pumping well locations.	12
15.	Flow chart for calibration process.	13
16.	Water-table elevations and observation well locations from 1964 USGS Hydrologic Atlas Series maps.	14
17.	Visual MODFLOW generated plot of observed and calculated water levels at observation well locations.	15
18.	Map showing 3-m water-table contour predicted by the calibrated model and observed water table.	16
19.	Differences in K in layer 1 between calibrated model and earlier model run.	17
20.	Differences in model predicted heads between layers 1 and 4, 1 and 6, 2 and 4, and 4 and 6.	18
21.	Map of model predicted drawdown.	19
22.	Illustrative example of two types of 5-year time-of-travel (TOT) areas predicted by model.	20
23.	Plot of normalized root mean squared (NRMS) error resulting from changes to K and R.	20
24.	Plot showing sensitivity of model predicted 5-year backward time-of-travel (TOT) capture zone areas to changes of K and R.	20
25.	Plot showing sensitivity of NRMS to inclusion of Manokin formation in the model.	20
26.	Map showing recommended WHPAs.	21

TABLES

Page

Table 1. Pumping well identifier, screen, and pumping rate information. . . . 3
2. Recharge and resource ratings and associated Kh, Kv, and K index values. . . . 8
3. Initial K values for material types observed in descriptive and geophysical logs. . . . 8
4. Areas assigned as constant head. . . . 9
5. Surface water bodies represented by river and drain boundaries. . . . 10
6. Recharge index numbers, values, and ratings. . . . 11
7. Recharge multipliers for land cover. . . . 13
8. Observation well Ids, locations, and average ground-water elevation. . . . 14
9. Effects of various no-flow boundaries representing saline ground water on NRMS. . . . 17

WELLHEAD PROTECTION AREA DELINEATIONS FOR THE LEWES-REHOBOTH BEACH AREA, DELAWARE

A. Scott Andres, Cheryl A. Duffy, and Evan M. Costas

ABSTRACT

Water supply in the rapidly developing Lewes and Rehoboth Beach areas of coastal Sussex County in Delaware is provided by more than 80 individual public water wells and hundreds of domestic wells. Significant concerns exist about the future viability of the ground-water resource in light of contamination threats and loss of recharge areas. As part of Delaware's Source Water and Assessment Protection Program, wellhead protection areas (WHPAs) were delineated for the 15 largest public supply wells operated by three public water systems.

The WHPAs are derived from analysis of results of dozens of steady-state ground-water flow simulations. The simulations were performed with a Visual MODFLOW-based 6-layer, 315,600-node model coupled with GIS-based data on land cover, ground-water recharge and resource potentials, and other base maps and aerial imagery. Because the model was operated under steady-state conditions, long-term average pumping rates were used in the model. The flow model includes four boundary types (constant head, constant flux, head-dependant flux, and no flow), with layers that represent the complex hydrogeologic conditions based on aquifer characterizations. The model is calibrated to within a 10% normalized root mean squared error of the observed water table.

The WHPAs are based on 5-year time of travel, that is, water reaching the water table will flow to a well within 5 years. In this study, the 5-year time of travel WHPAs are determined by backward and forward particle tracking methods. The recommended WHPAs are conservative in terms of water quality protection in that they incorporate the variations in the sizes of 5-year time of travel areas observed in the sensitivity analysis process. The resultant WHPAs for the Lewes and Rehoboth Beach areas cover almost 3.69 km^2.

INTRODUCTION

The study area is located in eastern Sussex County, Delaware (Fig. 1). This area has traditionally been known as a summer resort destination but there has been substantial development of outlet shopping centers and year-round housing over the past 15 years.

The area is entirely dependent on ground water for potable, commercial, and agricultural water needs. Potable water is supplied by over 80 public wells and hundreds of private domestic and commercial wells serving individual homes and businesses. The three largest public water systems serve an estimated population of over 100,000 people during peak demand times in the summer months (Andres and Talley, 2001). Water use by the Lewes Board of Public Works, Rehoboth Beach Water Department, and Tidewater Utilities, Inc. was evaluated from records on file at the Delaware Department of Natural Resources and Environmental Control (DNREC) and documented in a previous report (Andres and Talley, 2001). Well screen, pumping rate data, and locations of the 15 largest wells are shown in Table 1 and Figure 1, respectively.

Purpose and Scope

The Delaware Source Water and Assessment Protection Program (SWAPP) organized within the Ground Water Protection Branch of the DNREC, is charged with the responsibility to delineate wellhead protection areas (WHPAs) for public water supply sources, including public water wells, in Delaware (DNREC, 1990). WHPAs are recognized as sensitive water resource areas and are required by state law to be included in land use plans developed by counties and municipalities with more than 2,000 residents (Delaware Code, Chapter 92, Title 29).

Recognizing the complex hydrogeologic conditions and large number of wells in the study area and previous mapping and water quality work done in the area by the Delaware Geological Survey (DGS), SWAPP staff requested that the DGS conduct a study using digital ground-water flow models to delineate WHPAs for this area. The project proposal specified that the study would rely on existing data and publications from the DGS and DNREC. Following evaluations of hydrogeologic data and simple analytic model calculations, it was mutually agreed that ground-water flow modeling would be used to delineate WHPAs for public water systems that report pumping more than 190 m^3/day (50,000 gallons per day). Because of their limited impacts on ground-water flow, wells pumping smaller quantities of water are assigned simple 45-meter-radius (150 ft) WHPAs. This report documents the ground-water flow modeling efforts and results.

Previous Digital Flow Modeling Studies

Johnston's (1977) regional finite-difference model of the unconfined aquifer includes the Lewes and Rehoboth Beach areas. However, the model and results are not applicable in the current study because the large grid size (e.g., 1 square-mile blocks) and single layer used in the model do not allow for high-resolution computations of flow directions needed for WHPA delineations. Hodges' (1983) regional finite-difference model focused on ground-water flow in the confined Manokin and Pocomoke aquifers. Because the model grid consists of 1-square mile blocks and represents the unconfined aquifer as a constant-head boundary, the results are not applicable to this study.

Acknowledgments

This study was funded by the Delaware SWAPP and the DGS. We thank the Water Allocation Branch of the DNREC and the water utilities for providing background information on wells and water use, and Eric J. Trinkle, Steven M. Smailer, and Thomas E. McKenna for critically reviewing draft versions of the manuscript.

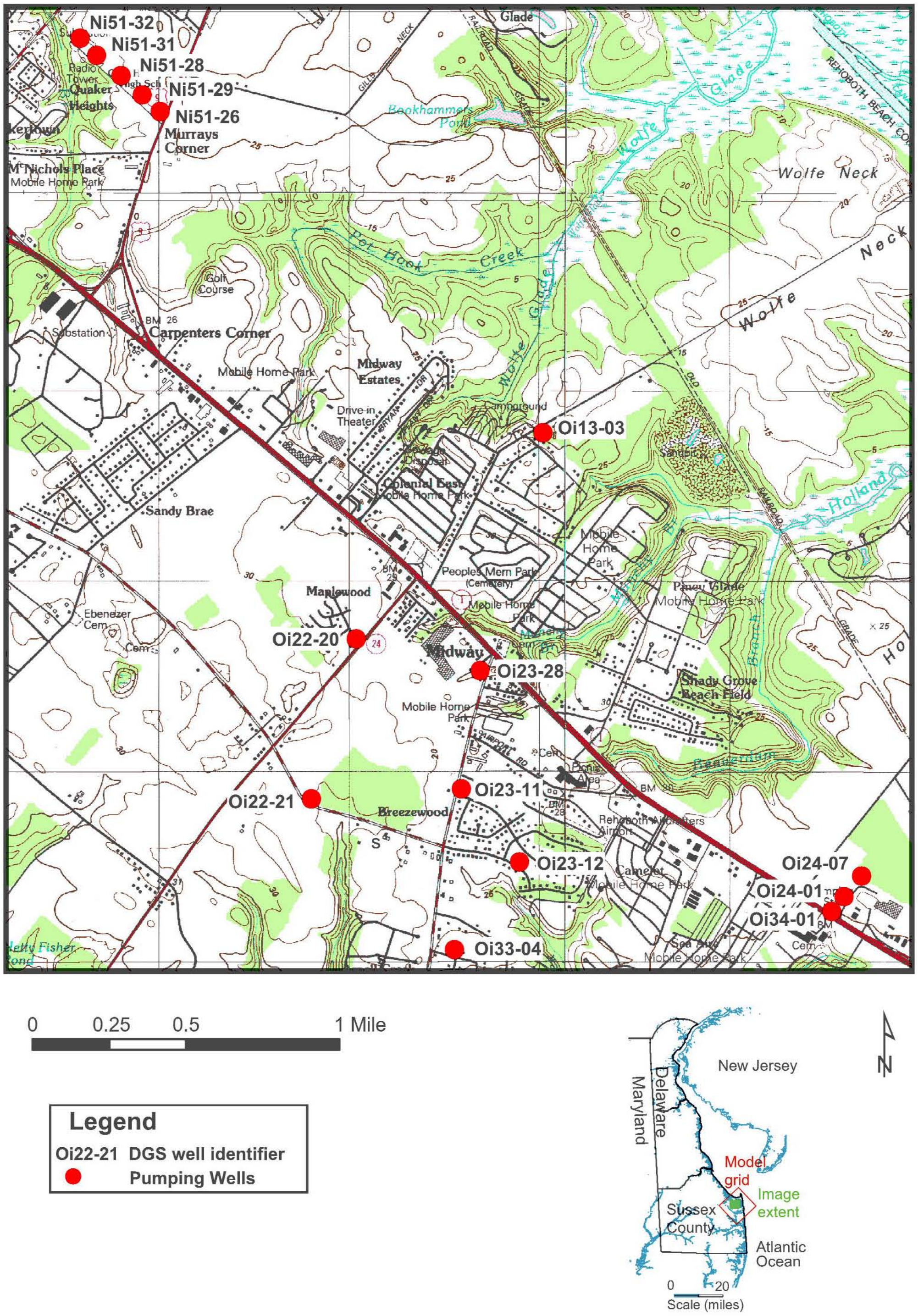

Figure 1. Location map of the study area and wellfields. Base map 1:24,000 digital raster graphic.

GENERAL HYDROGEOLOGY

This modeling study focuses on ground-water flow in the Columbia aquifer. The name Columbia aquifer has been used in a number of reports to describe the near-surface water-yielding sediments of the Delmarva Peninsula (Bachman, 1984; Bachman and Wilson, 1984; Andres, 1987; Talley, 1988). The name "Columbia aquifer" is derived from the Columbia Formation and Columbia Group as described in Delaware by Jordan (1962, 1964). Although Owens and Denny (1979), Groot et al. (1990), and Ramsey (1999, 2001, 2003) proposed different lithostratigraphic systems, and previous reports (Andres, 1987; Talley and Andres, 1987; Talley and Windish, 1984) on hydrologic units have also used the aquifer names Columbia-Pocomoke and Columbia-Manokin, the name Columbia aquifer is used in this report.

Application of the ground-water flow model to the hydrogeologic setting of the study area was guided by the geologic maps and nomenclature of Ramsey (1993, 2001, 2003), by hydrologic mapping and data compilation publications by Andres (1986, 1987) and Talley and Andres (1987), and by the results of ground-water recharge mapping pro-

Table 1. Pumping well identifier, screen, and rate information.

DGS Well ID	DNREC Permit No.	Screen Top (m)	Screen Bottom (m)	Rate (m^3/day)
Lewes				
Ni51-26	36869	-17	-50	2017.2
Ni51-29	45267	-31	-54	877.7
Ni51-28	50389	-17	-51	850.5
Ni51-31	55832	-26	-54	943.2
Ni51-32	55833	-17	-51	1172.1
Rehoboth Beach				
Oi34-01	10344	-14	-45	1308.4
Oi24-01	10345	-15	-36	1161.2
Oi23-12	2498	-23	-43	125.4
Oi24-07	36907	-14	-45	348.9
Oi23-11	38961	-19	-40	1303.0
Oi22-21	80761	-12	-31	1613.7
Tidewater Utilities				
Oi33-04	62677	-16	-37	81.3
Oi23-28	62742	-13	-32	298.1
Oi13-03	64923	-22	-40	444.3
Oi22-20	94743	-20	-38	445.6

jects covering the area (Andres 1991c; Howard and Andres, 1998; Andres and Keyser, 2001). Figure 2 is a generalized geologic map showing the distribution of surficial geologic units. Figure 3 is a northwest to southeast cross section showing the distribution of near-surface hydrologic units within the study area. The similar lithologies of the different lithostratigraphic units and lack of diagnostic fossils make their distinction uncertain on most driller, geologist, and geophysical logs; hence, the lithostratigraphic interpretations are conjectural. In general, Tertiary-age units thicken and dip to the southeast and Quaternary-age units thicken and dip eastward.

Lithostratigraphic Units and their Hydrologic Functions

Over much of Delaware, the Columbia aquifer is a complex hydrologic unit, usually consisting of two or more lithostratigraphic units and many lithofacies. At some locations in the study area the Columbia aquifer is vertically stratified into unconfined and leaky confined sections (Andres, 1986,1987). The known thickness of the Columbia aquifer is variable in the study area, ranging from a minimum of 15 m to a maximum of roughly 50 m. In the study area, the lithostratigraphic units in the Columbia aquifer, from lowermost to uppermost, are the Manokin, Bethany, Beaverdam, Lynch Heights, and Scotts Corners formations, and unnamed Holocene-age units.

There are complex facies relationships and boundaries between and among these units. Throughout the study area, the near surface deposits are very heterogeneous, ranging from estuarine silty sands, silt and sand, and sandy, clayey silts of Quaternary and/or Tertiary age, to shoreline sands deposited during Quaternary high stands of sea level and during the Holocene sea-level transgression. Low hydraulic conductivity (K) materials are associated with estuarine

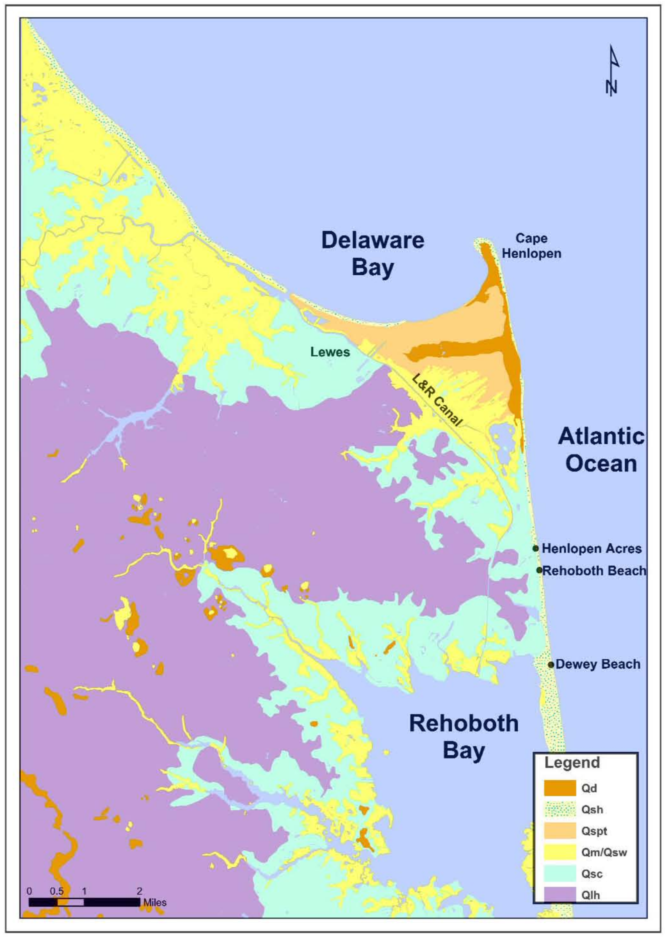

Figure 2. Generalized geologic map of study area. Geology modified from Ramsey (2003). Legend items are explained as: Qd – Dune deposits, Qsh – Shoreline deposits, Qspt – Spit, Qm/Qsw – Marsh and swamp deposits, Qsc – Scotts Corners Formation, Qlh – Lynch Heights Formation.

deposits and high K materials are associated with shoreline and tidal channel deposits. Discussions of depositional environments, mineralogy, and regional stratigraphy are contained in Benson (1990), Groot et al. (1990), Ramsey (1993, 1997, 2001, 2003), and Andres and Ramsey (1995, 1996).

Manokin Formation

The Manokin formation occurs only in the subsurface in the study area and dips and thickens toward the southeast. It is a heterogeneous unit consisting of interbedded olive gray to blue gray, fine to medium sand, silty fine sand, fine sandy silt, and less common beds of slightly gravelly, medium to coarse sand and sandy silty clay. Sandier beds form the Manokin aquifer. In the northernmost part of the study area, limited data indicate that sandy beds of the Manokin formation apparently function as part of the Columbia aquifer where they are in contact with sandy beds of the Beaverdam Formation. Over most of the study area, the Manokin aquifer is overlain by beds of fine-grained sediment and should have the properties of a confined aquifer. This aquifer is used for water supply by only a few domestic and irrigation wells in the study area because better quality water (i.e., lower iron concentrations) is available from higher yielding, shallower aquifers.

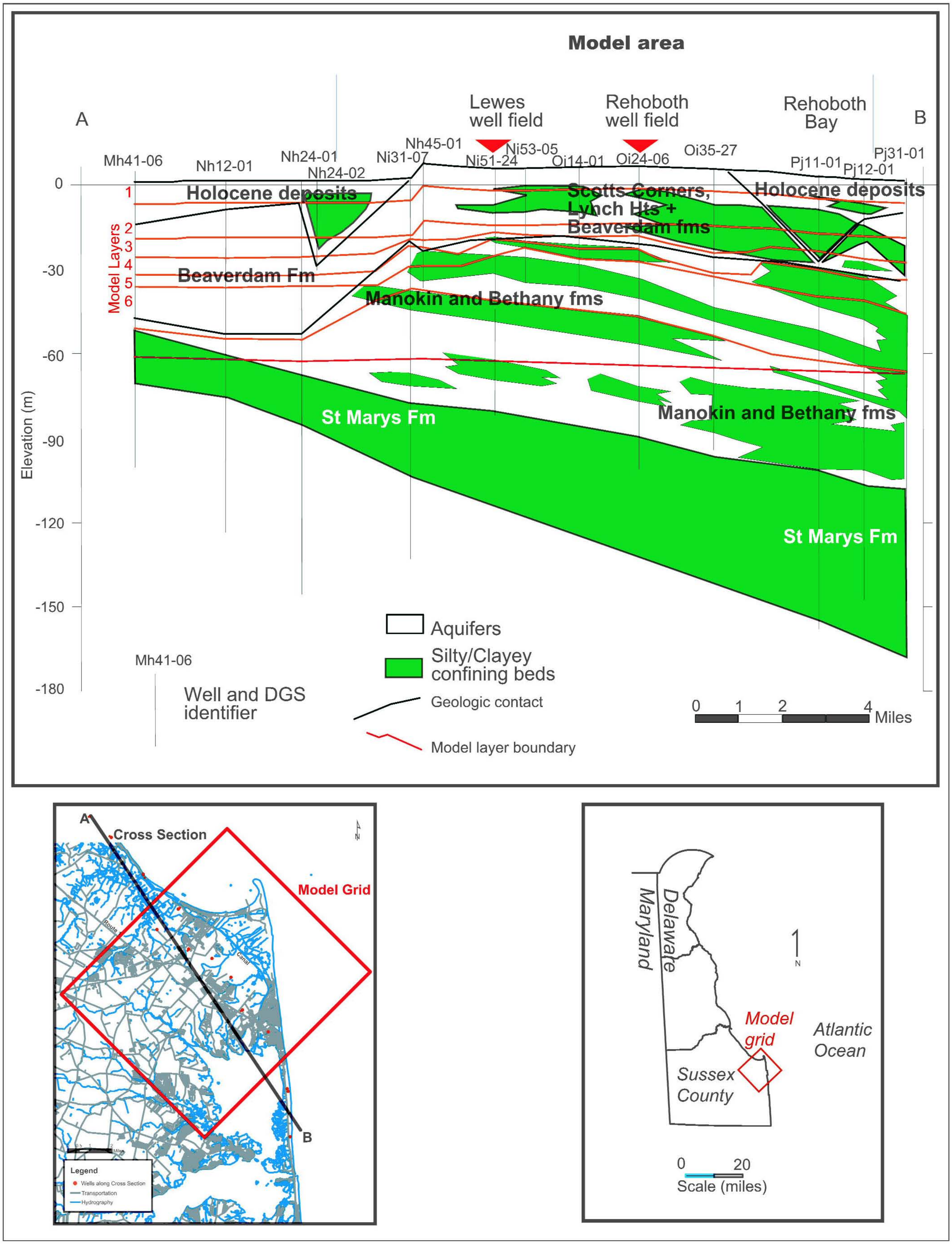

Figure 3. Cross-sectional hydrogeologic model (modified from Andres, 1986). This illustration depicts geologic and lithostratigraphic units and model layers.

Bethany Formation

Where present, the Bethany formation occurs at depths greater than 23 m. Our interpretation of geophysical and descriptive logs indicates that the Bethany is not present in the northernmost portion of the study area (north of the Lewes well field). Sand beds in the Bethany function as part of the Columbia aquifer in locations where they are in contact with sandy beds of the overlying Beaverdam Formation. The Bethany is a heterogeneous deposit consisting of interbedded olive gray to blue gray, fine sandy silt, sandy silty clay, silty fine sand, fine to medium sand, and rare beds of slightly gravelly medium to coarse sand. Wells owned by the City of Lewes withdraw water from the Bethany formation.

Beaverdam Formation

The Beaverdam Formation is not exposed at the surface in the study area but occurs at shallow depths and functions as part of the Columbia aquifer. Over much of the study area, the Beaverdam occurs within 6 m of land surface where it is a very pale orange to moderate yellow-brown, medium to coarse sand with beds of gravelly coarse sand, silty fine sand, fine sandy silt and/or clay (Andres, 1987; Ramsey, 2001, 2003). Scattered thin layers of dark-colored silty clay and clayey silt are present throughout. The very pale orange color, distinctive multicolored coarse sand grains, weathered and friable lithic fragments, and sticky coatings on grains distinguish the Beaverdam from younger units. The Beaverdam unconformably overlies the Manokin and Bethany formations and is interpreted to have been deposited in near-shore marine, estuarine, lagoonal, and fluvial environments (Ramsey, 2001; Andres and Ramsey, 1996; Groot and Jordan, 1999). Sandier beds in the Beaverdam function as part of the Columbia aquifer, and most water-supply wells obtain water from these beds. Fine-grained beds function as confining units.

Lynch Heights and Scotts Corners Formations

The study area includes the outcrop area of the Lynch Heights and Scotts Corners Formations (Ramsey and Schenck, 1990; Ramsey, 2001, 2003). These units are recognized in logs and exposures as a medium to fine sand with admixtures of silt and clay matrix and rare beds of gravelly coarse sand. Shells and shell fragments are rarely noted. The Scotts Corners, Lynch Heights, and Beaverdam consist of sediments deposited in similar estuarine, lagoonal, and near-shore marine environments, so they have similar lithologies. In some locations fossil pollen assist in the identification of stratigraphic units and recognition of unconformities. Geologic mapping of the Lewes and Cape Henlopen quadrangles (Ramsey, 2003) has found that lithologic distinctions between sands of the Lynch Heights and Scotts Corners Formations and Holocene beach deposits are not clear, and differentiation between these units is made using geomorphic criteria. Sandier beds in these units function as part of the Columbia aquifer. Fine-grained beds function as confining units.

Shoreline Deposits

Sand units found at the margin of the coastline are recognized as an informal lithostratigraphic unit. Ramsey (1999; 2003) interprets these units as sediments deposited in beach, dune, back-dune, and washover environments during the Holocene transgression. They have variable thickness; some are less than 6 m thick around Rehoboth Beach and Dewey Beach. Thicker units, as much as 18 m, are found in the beaches north of Henlopen Acres. Where thickness exceeds 6 m, these areas are excellent recharge areas. The sands along the Delaware Bay have fair recharge-potential ratings because they are not as thick and because silty sands and mud units underlie them. These mud units may be remnants of an older Delaware Bay bottom (Ramsey, 2001; 2003).

Marsh and Swamp Deposits

Marsh and swamp deposits are recognized as an informal map unit. Marsh deposits are found along the margins of Rehoboth and Indian River bays, tributary tidal creeks, and along the Lewes and Rehoboth Canal. Swamp deposits are found in locations fringing the marsh deposits, in riparian zones fringing non-tidal fresh-water streams, and in undrained depressions associated with inland dune deposits. Swamp deposits are differentiated from marsh deposits by their tree cover. Both marsh and swamp deposits consist of sandy, organic-rich silts, and silty sands. They range in thickness from less than 0.3 m to about 3 m, and unconformably overlie older units. Marsh and swamp deposits interfinger with each other and with other Holocene-age shoreline and other coastal deposits. Because of their fine-grained character, marsh and swamp deposits usually function as confining beds.

Dune Deposits

Dune deposits are found in two general areas, one in the coastal zone associated with Cape Henlopen, and the other in inland locations. Dune deposits usually consist of fine to medium sand with scattered thin beds of silty fine sand, and, because of this sandy character, they should readily transmit water. Dune deposits located along the coast are of Holocene age (Ramsey, 2001; 2003), and unconformably overlie Pleistocene and older units. These coastal dune deposits range in thickness from 1 m to over 30 m and interfinger with beach, swamp, and marsh deposits. Dune deposits, recognized by their distinctive geomorphology, also occur in inland areas overlying both the Scotts Corners and Lynch Heights Formations. The age or ages of dune deposits in inland areas and their stratigraphic relationships with the Scotts Corners and Lynch Heights Formations are unknown. They range in thickness from 1 m to just over 6 m.

Man-made Deposits

There are some land areas in the study area that are underlain by dredge spoils, such as along the Lewes and Rehoboth Canal and smaller canals adjacent to Rehoboth Bay.

Aquifer Tests

Results of a limited number of aquifer tests, most of which were conducted for the Lewes and Rehoboth Beach wells (Johnston, 1977; Hodges, 1983; Andres, 1986; Talley and Andres, 1987), show a wide range of values of transmissivity. Tests typically were of durations shorter than 48 hours and used one or no observation wells, conditions that limit the applicability, accuracy, and reliability of the results. The test data are limited to only a few widely spaced locations; hence, extrapolation of this data to untested areas is of questionable validity. The hydraulic properties derived from aquifer tests are representative of an aquifer thickness represented by multiple layers in the modeling software. Because of these limitations, aquifer test data are not a primary source of hydraulic property data.

Ground-Water Levels

The maps of Adams et al. (1964) and Boggess et al. (1964) show estimated water-table elevations in the forms of points and contours. They are the primary data sources for evaluating model performance. The point data also include ranges of observed water-table elevations measured between 1958 and 1961. It is important to note that the accuracy of the information cannot be verified because the original depth-to-water and well construction data for most of these observation points cannot be located. Procedures for evaluating and correcting these data are discussed in following sections.

Additional ground-water levels have been measured in wells scattered over the study area and are presented by Hodges (1983), Talley and Andres (1987), Andres (1991d), and in additional data that are in DGS files. While the temporal distribution of the measurements are adequate for evaluation of temporal trends at individual locations the limited spatial distribution of the wells is not adequate for evaluation of model performance in this study.

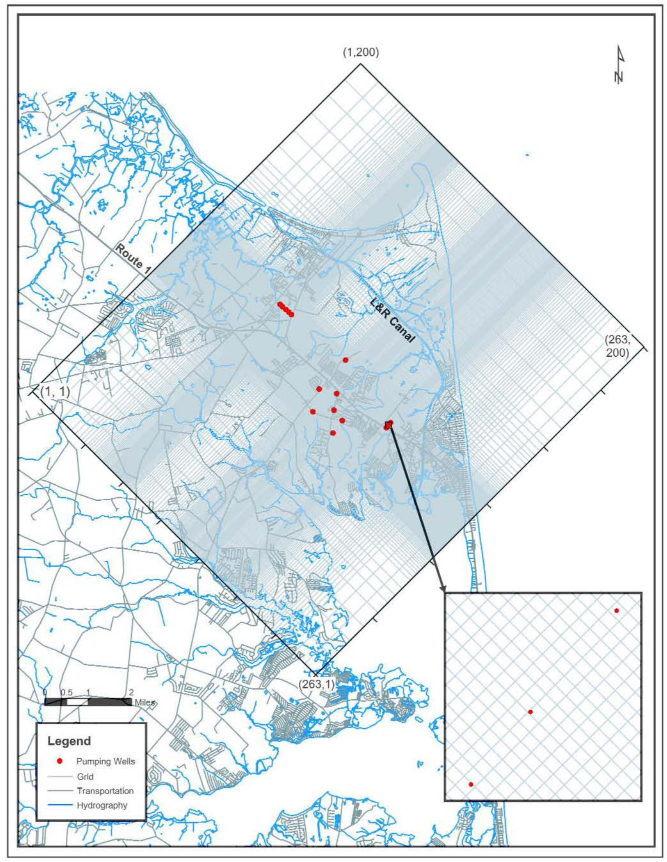

Figure 4. Map of model grid and study area. Base map data from Delaware DataMil (www.datamil.udel.edu). Grid inset indicates cells sizes approximately 15 meters around pumping wells.

METHODS

Model Implementation

Digital ground-water models are representations of the real world converted to mathematical formulae and numerical data on hydrogeologic conditions. Data input to the formulae include locations of pumping wells with associated pumping rates and screen depth information for each well; locations of observation wells and associated elevations of the water table; thickness and hydraulic properties of subsurface units; recharge rate; and boundaries (e.g., constant head, no flow, head-dependent flux, and constant flux). Visual MODFLOW (Waterloo Hydrogeologic Inc., 2002) is the computer program used in this study to conduct finite-difference simulations and modeling of three-dimensional ground-water flow and contaminant transport. Visual MODFLOW is a proprietary software product based upon the U. S. Geological Survey MODFLOW (MacDonald and Harbaugh, 1988) software. Visual MODFLOW includes pre- and post-processing modules to allow the modeler to control data entry and displays of simulation output with a graphic interface.

In this study, a steady-state, 6-layer, numerical model simulates hydrogeology and ground-water flow in the Lewes and Rehoboth Beach areas in Sussex County, Delaware. The model does not simulate effects of seasonal and yearly changes in recharge and withdrawal. However, because steady-state models predict long-term conditions, steady-state simulations are an efficient and resource-conservative approach for defining WHPAs.

Simulation of ground-water flow with a finite-difference model requires the model area to be represented by a grid (MacDonald and Harbaugh, 1988). The model grid used in this study has 263 rows, 200 columns, and six layers. To take advantage of the clustering of wells along Route 1 (Fig. 1), and to reduce the number of grid cells, grid blocks are of variable sizes and the grid rotated forty-five degrees from north (Fig. 4). The smallest cell sizes are 15 m by 15 m in the areas of the pumping wells. In order to reduce computation and data manipulation times for the simulations, grid cell sizes are increased with distance from each cluster of wells (MacDonald and Harbaugh, 1988; Hinaman and Tenbus, 2000), with the maximum change in size between adjacent cells no greater than 1.5. The largest model cells around the edge of the grid are approximately 1000 m by 1000 m.

Layer delineations reflect results of previous mapping and hydrologic studies listed in previous sections. These studies found that individual sedimentary units are areally discontinuous and have complex geometries because of facies changes and erosional unconformities (Andres, 1987; Ramsey, 1999, 2001, 2003). A schematic cross section (Fig. 5) illustrates how the six layers of the model represent the complex hydrogeologic conditions.

Land surface in the model was derived from the 30-meter digital elevation model (DEM) of the University of Delaware's Spatial Analysis Lab, developed by John Mackenzie (http://www.udel.edu/FREC/spatlab/). Because the model grid blocks are not the same configuration as the DEM

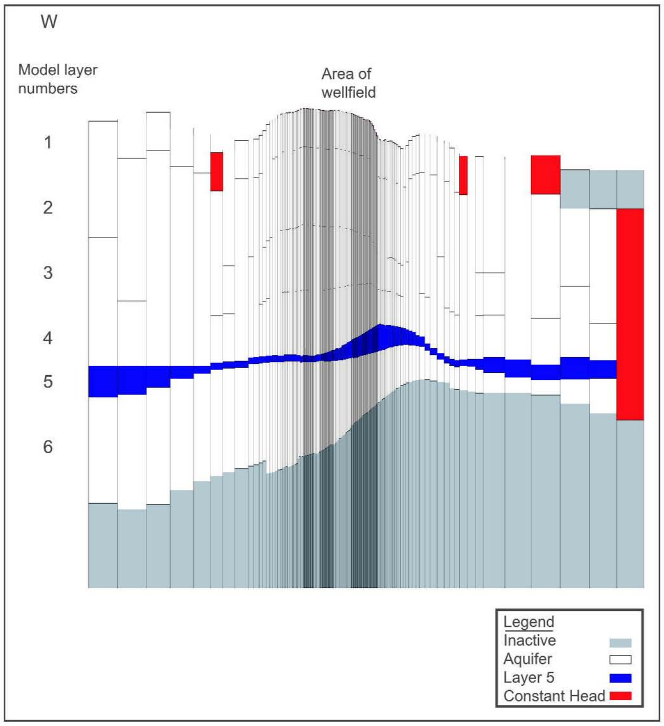

Figure 5. Cross-sectional view of model grid along row 113. Layer 5, which represents a discontinuous confining bed, is shaded blue.

grid, Visual MODFLOW uses the block-average land surface elevations for each model grid block for computations.

Layer 1 extends from land surface to 6 m below the surface and corresponds with the interval mapped in ground-water recharge potential projects (Andres, 1991a, b; Howard and Andres, 1999; Andres and Keyser, 2001). Interpretations of the composition of sediments in boreholes and exposures determine whether recharge potential is identified as excellent, good, fair, or poor. In general, sandiest sections are rated excellent, with a lessening of recharge potential with increasing abundance of clay and silt. Single-well aquifer tests from over 200 monitoring wells characterize the relationship between sediment composition and hydraulic conductivity, and, hence, between recharge potential and hydraulic conductivity (Andres, 2003; DGS files).

Layer 2 extends from 6 m below the surface to 18 m below the surface. It corresponds to the resource interval described in Andres (1991a). Methods similar to those used to characterize hydraulic properties for layer 1 are used to characterize hydraulic properties of layer 2.

The geometries of layers 3 and 4 represent the interval extending from the bottom of layer 2, at 18 m below the surface, to the base of the Columbia aquifer (Andres, 1987) or –30 m NAVD 1988 (North American Vertical Datum of 1988), whichever is shallowest. The two conditions defining the base of layer 4 represent the discontinuous character of the confining units that form the base of the aquifer. Layers 3 and 4 correspond to the upper and bottom halves of this interval, respectively. This geometry is used to increase the vertical resolution of the model.

A grid of elevations of the base of layer 4 was interpolated on a 30-meter grid with Surfer 7 (Golden Software, Inc., Golden, CO) on the bases of data from Andres (1987) and more recent point data from the Delaware Geological Survey's files. Visual MODFLOW was used to compute block-average elevation values for the model grid blocks from the Surfer grid.

Layer 5 represents spatially discontinuous confining units that, where present, form the base of the Columbia aquifer. The bottom of layer 5 is either the base of the confining unit or 3 m below the top of layer 5.

Layer 6 represents the remaining thickness of unconfined and semi-confined Columbia aquifer, the shallowest semi-confined Pocomoke aquifer, and associated confining units. It extends from the base of layer 5 to either the base of this aquifer or to –53 m NAVD 1988, whichever is shallowest. Because layer 6 is the lowermost layer in the model, the base of layer 6 is a no flow boundary.

Adding an additional layer to the base of the model tested the effect of representing the base of layer 6 as a no-flow boundary (see Sensitivity Analysis section). This layer extends from the base of layer 6 to a uniform bottom elevation for the entire grid at approximately –65 m. This additional layer represents the numerous fine-grained beds in the lower Bethany and upper Manokin formations. This layer is modeled as a no-flow boundary to reduce the complexity of the model. The fine-grained character of these materials and the limited pumping from the underlying Manokin aquifer in the study area are thought to limit the flow of water between the Manokin aquifer and overlying Columbia and Pocomoke aquifers.

Hydraulic Conductivity

The model represents hydraulic conductivity (K) as spatially heterogeneous and anisotropic, that is, K varies from cell to cell in the model as well as directionally within each cell. For computational and storage efficiency, K data are input to Visual MODFLOW as matrices of integer index values corresponding to discreet K values stored in a separate table. Because there are no data to indicate otherwise, horizontal hydraulic conductivity (Kh) is assumed to be isotropic. In sedimentary rocks where bedding is near horizontal, grain packing causes vertical hydraulic conductivity (Kz) to be less than Kh (Freeze and Cherry, 1979). Following rule-of-thumb guidance in the literature, model Kz varies from 5 to 10 percent of Kh and the magnitude of vertical anisotropy increases with decreasing Kh (Anderson and Woessner, 1992; Freeze and Cherry, 1979).

Conductivity values were assigned to layers 1 and 2 (figures 6 and 7) on the bases of recharge and resource maps (Andres, 1991a, b; Howard and Andres, 1999; Andres and Keyser, 2001) and K index values associated with each recharge and resource rating (Table 2). These maps were converted to 30-meter grids using the ArcToolbox 8.2 (ESRI, Inc., Redlands, CA) polygon to grid function and converted to block-average K values. For layers 3 through 6 (figures 8-10), K values were estimated from geophysical or lithologic descriptive logs. The thickness (b) of sand, silty sand, mud, and interbedded mud and sand were determined for each log for the depth intervals corresponding to the model layers. K values were assigned for each material type (Table 3) and a single K value was computed for each model layer using the equation:

$$((K1 \times b1) + (K2 \times b2) + ... + (Kn \times bn)) / (b1 + b2 + ... + bn)$$

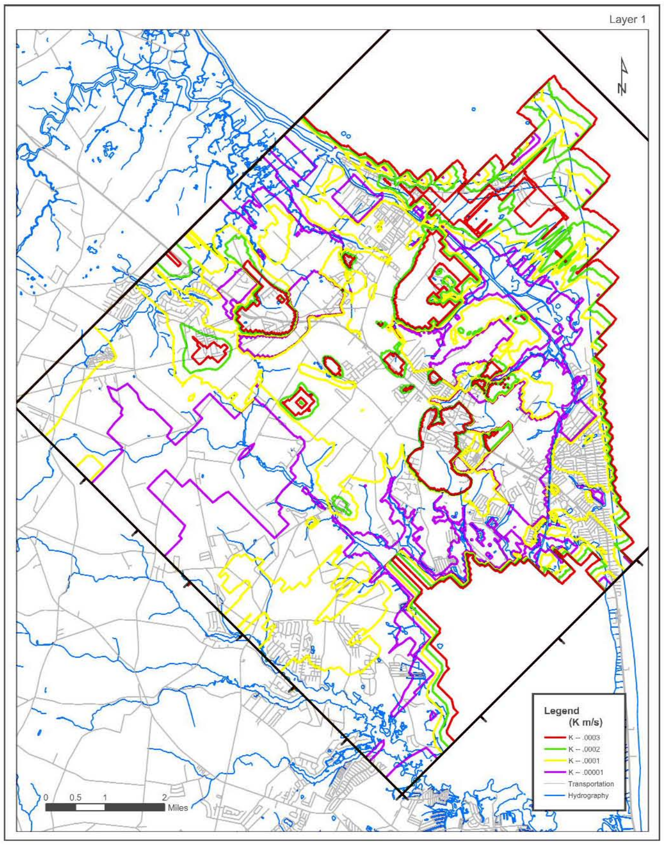

Figure 6. Map showing spatial pattern of K (m/s) for layer 1. K determinations are guided by ground-water recharge potential maps and recharge mapping methodology (Andres, 1991a, 1991c; Howard and Andres, 1999; Andres and Keyser, 2001).

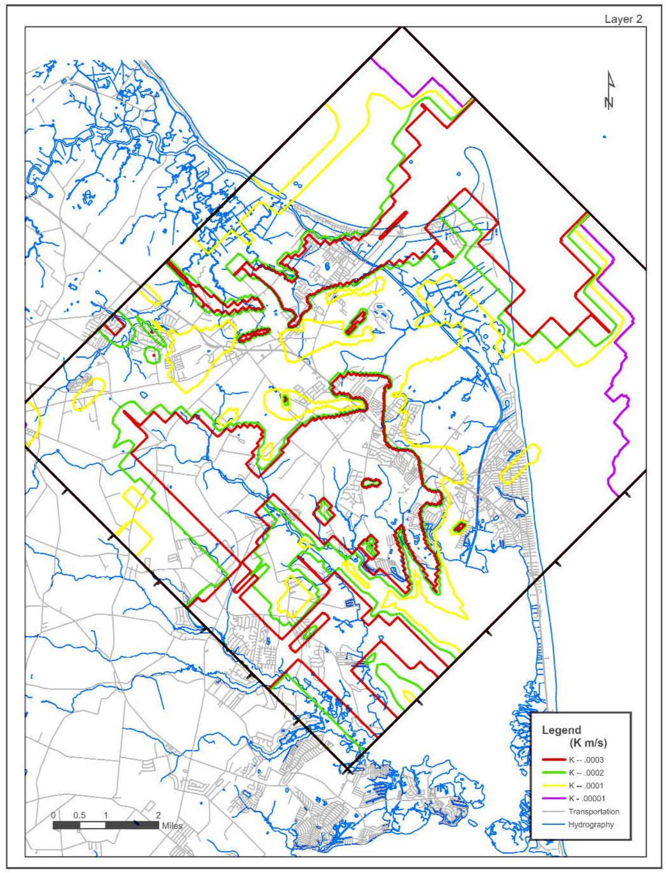

Figure 7. Map showing spatial pattern of K (m/s) for layer 2. K determinations guided by ground-water resource potential maps (Andres, 1991a; this study).

Table 2. Recharge and resource ratings, and associated Kh, Kv, and K index values.

K index	Kv (m/s)	Kh (m/s)	Recharge Potential Category (RPC)
1	3.65E-5	0.0003648	Excellent
2	3.04E-5	0.000304	
3	2.64E-5	0.000264	
4	2.24E-5	0.000224	
5	1.92E-5	0.000192	Good
6	1.52E-5	0.000152	
7	1.36E-5	0.000136	
8	5.6E-6	0.000112	
9	4.8E-6	9.6E-5	Fair
10	3.6E-6	7.2E-5	
11	3.2E-6	6.4E-5	
12	2.1E-6	5.6E-5	
13	7.5E-7	2E-5	Poor
14	6E-7	1.6E-5	
15	3E-7	8E-6	
16	4.5E-8	1.2E-6	

The point K values were then assigned a K index value using the ranges shown in Table 2. A 30-meter K index grid was computed with Surfer for each layer. Gridding parameters were inverse-distance squared, quadrant search, 2 nearest neighbors with 1 neighbor per quadrant, and a 2000-meter search radius. Visual MODFLOW computed the block-averaged K index values for the model's grid cells.

Table 3. Initial K values for material types observed in descriptive and geophysical logs.

Material type	K value (m/s)
Sand	0.000347
Silty sand	0.000174
Mud	0.000017
Interbedded sand and mud	0.000093

Boundary Conditions

For all steady-state simulations, at least one boundary must act as a reference pressure, or head, for all calculations (MacDonald and Harbaugh, 1988). Four types of boundary conditions are incorporated into this model: constant head (Table 4), constant flux (recharge and pumping), head-dependant flux (rivers and drains), and no flow (figures 11 and 12). In all MODFLOW models the entire model is surrounded by no-flow boundaries.

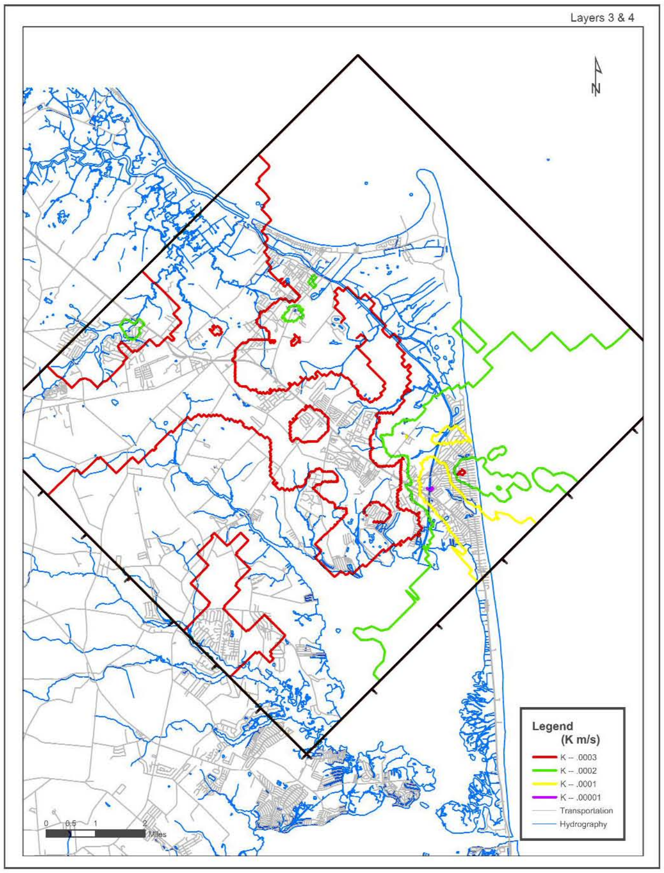

Figure 8. Map showing spatial pattern of K (m/s) for layers 3-4. K determined from irregularly distributed borehole lithologic description data.

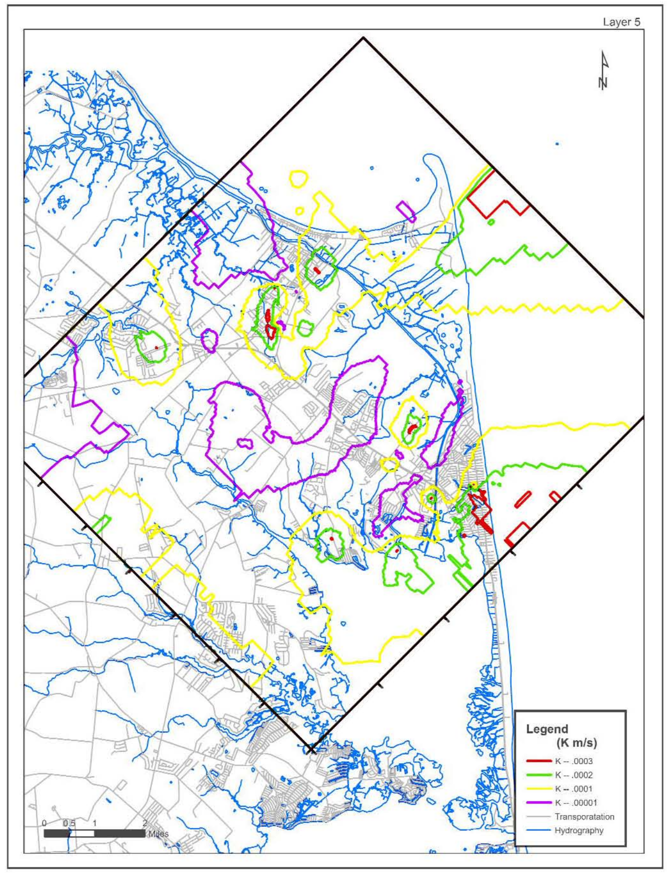

Figure 9. Map showing spatial pattern of K (m/s) for layer 5. K determined from irregularly distributed borehole lithologic description data.

Table 4. Areas assigned as constant head.

<u>Head set by water depth</u>
• Delaware Bay
• Atlantic Ocean
<u>Head set to mean water level of Rehoboth Bay</u>
• Rehoboth Bay
• L&R Canal
<u>Head set to mean water level of Rehoboth Bay +0.1m (tidal areas)</u>
• Love Creek
• Arnell Creek
• Bald Eagle Creek
• Old Mill Creek
• Great Marsh Area
• Holland Glade
• Wolfe Glade
<u>Head set to elevation shown on USGS 1992 topographic map</u>
• Red Mill Pond

Because Visual MODFLOW does not simulate density-dependent ground-water flow, boundaries representing bodies of saline surface water are approximated by a combination of two boundaries: constant-head boundaries at model cells representing the landward edges of bodies of saline surface water and no-flow cells in the immediately adjacent cells. Anderson and Woessner (1992), Hinaman and Tenbus (2000), and Reilly (2001) present discussions of this approximation in more detail. Several different configurations of this type of boundary were tested. The first general type of configuration approximates a condition where flow in layer 1 encounters the constant-head-no-flow boundary at the coastline (Fig. 11), and flow in layers 2 through 6 moves under the coast to constant head-no flow boundaries located offshore (Fig. 12). A second configuration approximates a condition where layers 2 through 4 are saturated with saline water beneath Delaware Bay and the Atlantic Ocean and are represented by the coastline boundary shown in Figure 11, and fresh ground water in layers 5 and 6 can flow to discharge areas located offshore (Fig. 12). Additional tests were run with no-flow boundaries in layers 2-4 in cells under Rehoboth Bay and in cells under the Lewes and Rehoboth Canal.

Model cells corresponding to bodies of fresh surface water are represented as constant head or head-dependent flux boundaries. Constant head cells were assigned to cells representing bodies of fresh surface water controlled by a dam (e.g., Red Mill Pond). Head-dependent flux boundaries, where flow across a head-dependent flux boundary depends on the difference between a user-supplied specified head and the model-calculated head on either side of the boundary (Anderson and Woessner, 1992), represent all other freshwater streams.

Rivers and drains are the two types of head-dependent flux boundaries in the model. The main difference between rivers and drains is that river cells can add unlimited quantities of water to the aquifer when the river stage falls below the

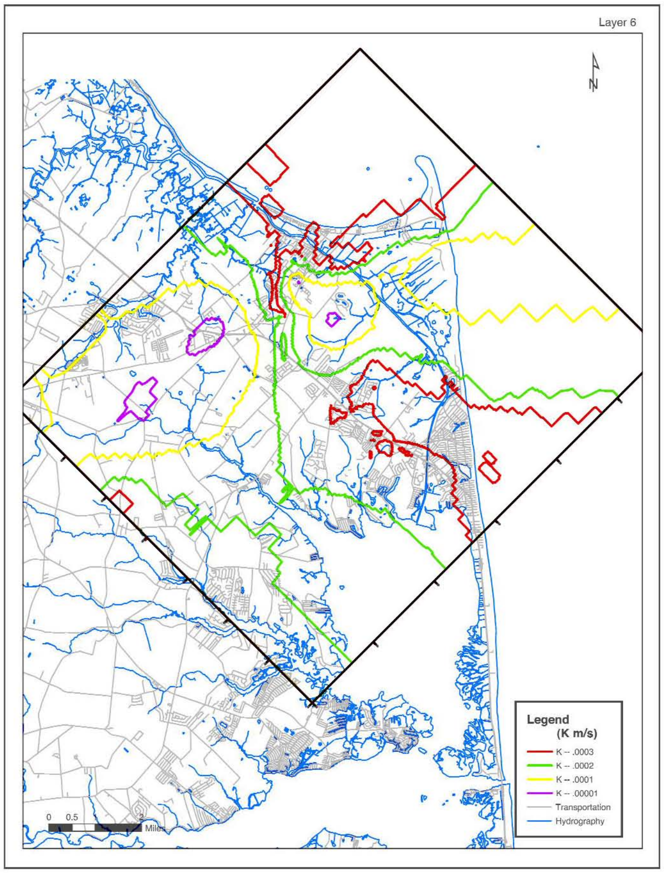

Figure 10. Map showing spatial pattern of K (m/s) for layer 6. K determined from irregularly distributed borehole lithologic description data.

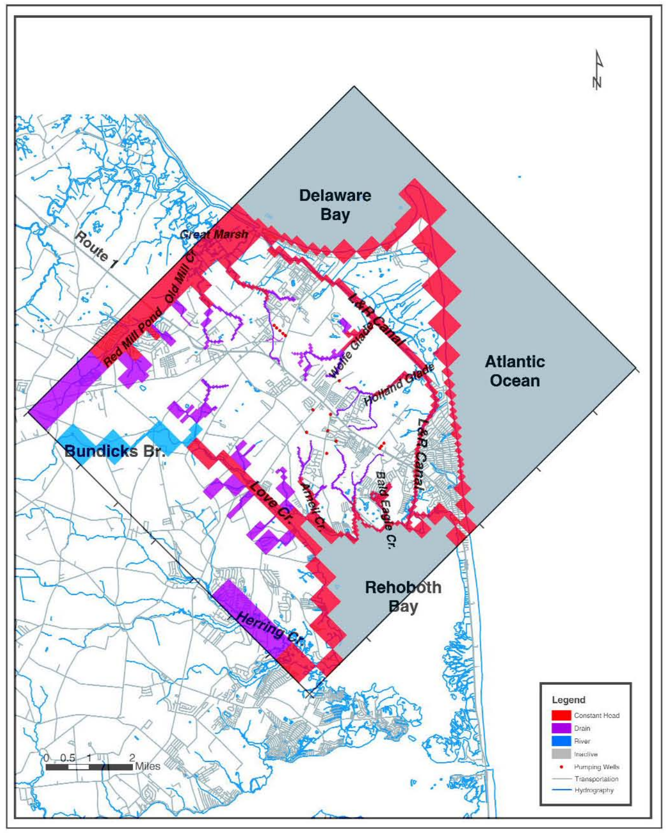

Figure 11. Map of model boundary cells for layer 1. Several approximations of the ocean, bay, and canal boundaries were tested.

Table 5. Surface water bodies represented by river and drain boundaries.

Rivers	Drains
Bundicks Branch	Herring Creek
	Cherry Walk Creek
	Stillman Glade
	Goslee Creek
	Hetty Fisher Glade
	Dorman Branch
	White Oak Creek
	Johnson Branch
	Beaverdam Branch
	Munchy Branch
	Wolfe Glade
	Pot Hook Creek
	Gills Neck
	Ebenezer Branch
	Canary Creek
	Black Hog Gut

head in the aquifer. River boundary cells require input data on river stage (elevation of the water surface), river-bottom elevation, and river-bottom conductance. River-bottom conductance represents the resistance to flow between the surface water body and the ground water (MacDonald and Harbaugh, 1988). Bundicks Branch (Fig. 11) is the only stream in the study area designated as a river boundary in the model.

Cells defined as drains act only as sinks of water, meaning there is no leakage of water from drain cells to aquifer cells when heads in aquifer cells are less than the heads in drain cells (Anderson and Woessner, 1992). The rate at which drains remove water is proportional to the difference between the head in the aquifer and the fixed elevation of the bottom of the drain (Waterloo Hydrogeologic Inc., 2000). Similar to river boundaries, the model uses elevation and conductance data to compute the amount of water flowing to a drain. Field observations of no-flow during dry summer months are the basis for assigning drain boundaries to a number of small streams (Table 5, Fig. 11).

Recharge (R) is water that enters the ground-water system (Freeze and Cherry, 1979). In the model, however, only R derived from infiltration of precipitation is included in the simulation and is input to the topmost saturated layer. Recharge due to wastewater discharge is not included in the model. Johnston (1973, 1976, 1977) reports average recharge rates of 330 to 407 mm/yr to the unconfined Columbia aquifer. Later aquifer testing and simulation work by Andres (1991a, b) and Andres and Brough (1994) refined areal recharge rates on the bases of aquifer material properties and numerical simulations. These improved recharge values are used as input to the model (Table 6, Fig. 13).

In addition to aquifer properties, structures built on land surface also affect R. For example, where a sandy aquifer would allow a large amount of water to percolate through the surface, pavement and buildings over the area force the water to flow laterally over the surface to a stream,

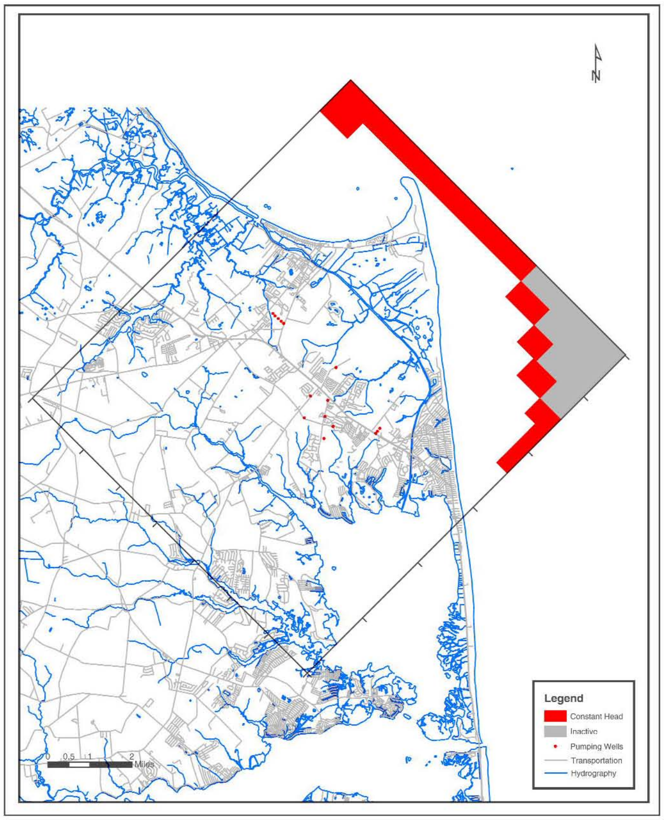

Figure 12. Map of model boundary cells for layers 2-6. Several approximations of the ocean, bay, and canal boundaries were tested.

Table 6. Recharge index numbers, values, and ratings.

Index #	Recharge (mm/yr)	Recharge Potential Category (RPC)
2	492	Excellent
3	469	
4	446	
5	423	Good
6	400	
7	311	
8	292	
9	273	Fair
10	254	
11	235	
12	216	
13	197	Poor
14	178	
15	159	
16	140	

retention basin storm drain, or some other engineered structure. Based on the categories of the USGS's standard land use – land cover (LULC) classification system (Anderson et al., 1976), land-use and land-cover are represented in the model as a recharge multiplier. The formula is:

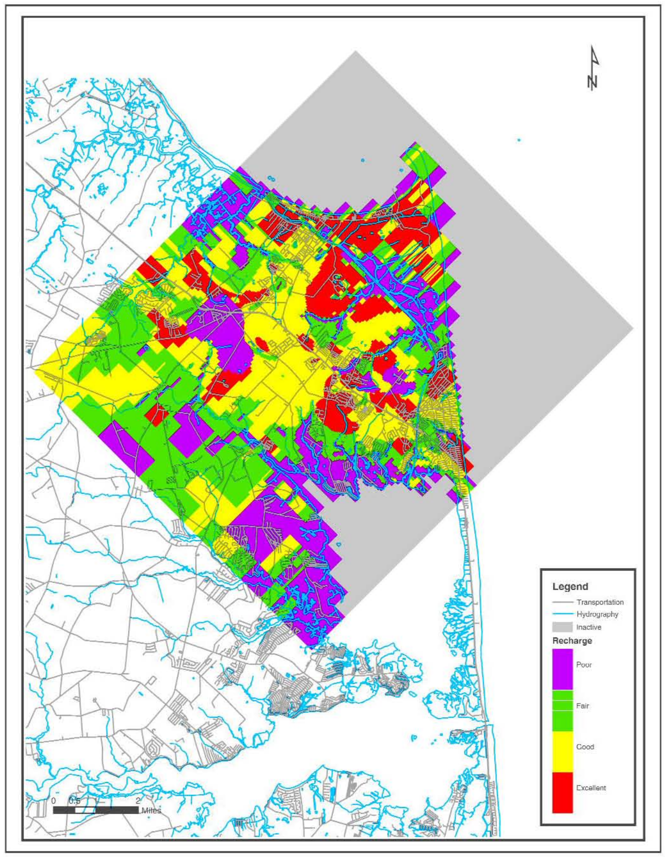

Figure 13. Map showing spatial pattern of recharge for uppermost active layer. R determinations are guided by ground-water recharge potential maps and methodology (Andres, 1991a, 1991c; Andres and Brough, 1994; Howard and Andres, 1999; Andres and Keyser, 2001).

Post-development R = (Pre-development R) * (1 – % impervious LULC).

Table 7 shows ten land-cover categories (Anderson et al., 1976) and percent impervious cover for those categories from the Water Resources Agency at the University of Delaware (http://www.wr.udel.edu/).

The model represents pumping wells as constant flux boundaries. We included fifteen public water supply wells in the model, six owned by the City of Rehoboth Beach, four by Tidewater Utilities, and five by the City of Lewes (Fig. 14, Table 1). Input data consists of pumping rates and the elevation of the top and bottom of each well screen.

Model Calibration

Calibration is the process in which model input data are adjusted so that field-measured heads and/or flows are reproduced through model simulations within an acceptable range of error (Anderson and Woessner, 1992). Common criteria for an acceptable calibration are a normalized root mean squared (NRMS) error equal to or less than 10 percent (Hinaman and Tenbus, 2000) and visual matching of observed and predicted water-table contours. NRMS error is a statistical measure of the differences between observed and predicted values at point locations. Although a calibrated model is then a reasonable representation of real-world conditions, it is not a unique solution because of the number of variables that can be adjusted in the calibration process (Anderson and Woessner, 1992).

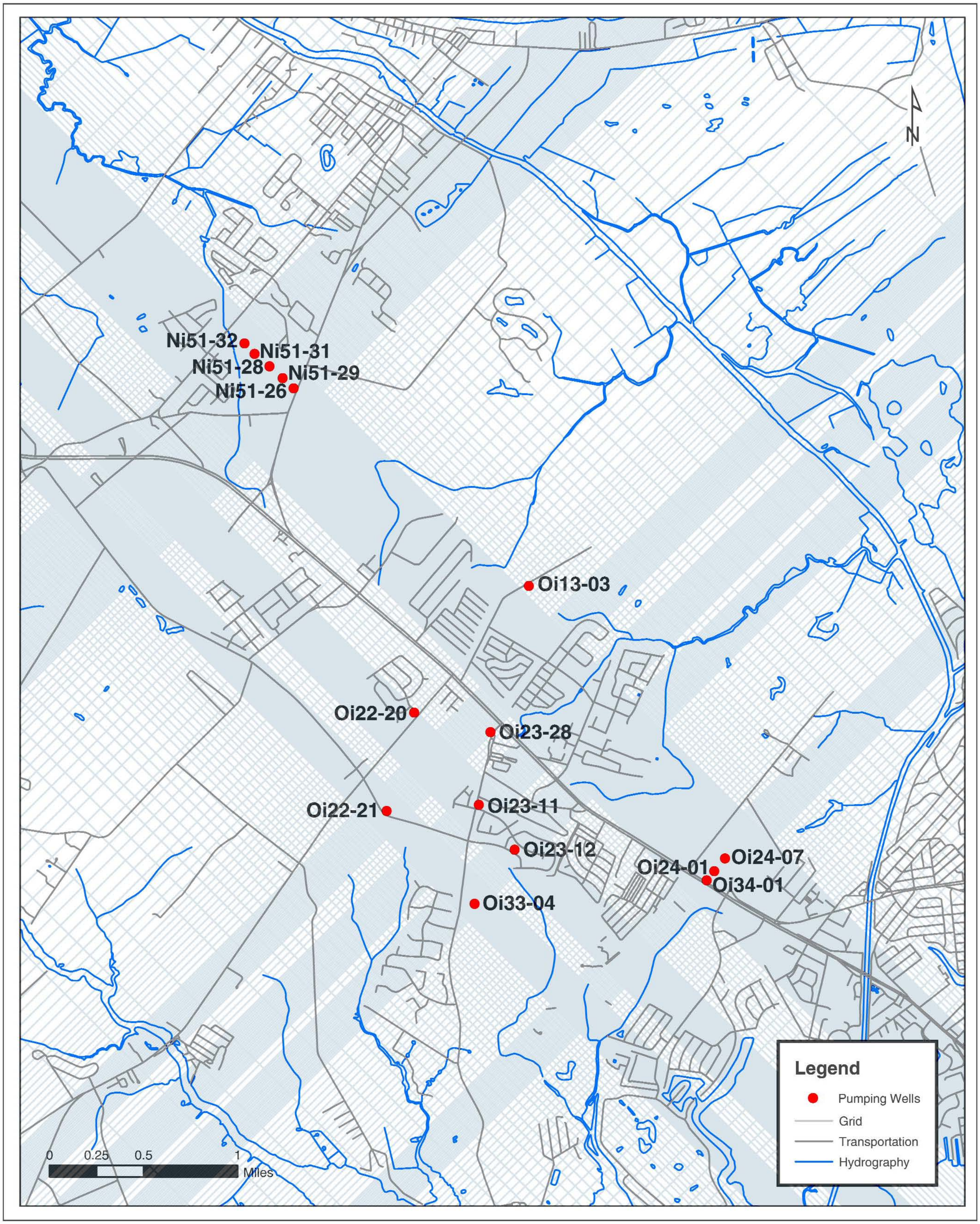

Figure 14. Map showing pumping well locations.

Table 7. Recharge multipliers for land cover (LC). Percent impervious determined by the University of Delaware's Water Resources Agency.

LC Group	% Impervious Surface	Recharge Multiplier
Single Family Dwellings	30	0.7
Multi-Family Dwellings	65	0.35
Commercial-Industrial	85	0.15
Transportation	90	0.1
Urban	85	0.15
Agriculture	0	1.0
Rangeland-Forest	0	1.0
Water Area	0	1.0
Sandy Area	0	1.0
Transitional	0	1.0

In this study, the model calibration process consisted of trial-and-error adjustments to conductivity, recharge, and properties of constant head, drain, and river boundaries (Fig. 15) to approximate water-table elevations (Fig. 16, Table 8) from Adams et al. (1964) and Boggess et al. (1964). There are no long-term stream discharge data with which to calibrate flow. Upper and lower bounds on the range of K values are derived from aquifer test data (Andres, 1991a, 2003; Talley and Andres, 1987) and other data relating material types to K (Freeze and Cherry, 1979). Upper and lower bounds on the range of R are from water-budget data (Johnston, 1973, 1976, 1977; Andres and Brough, 1994).

Adjustments To Calibration Dataset

The accuracy of water level data used to calibrate the model was evaluated during the calibration process. Comparison of land elevations from the Lewes, Cape Henlopen, Fairmount, and Rehoboth Beach 7.5-minute quadrangles (U. S. Geological Survey, 1991a–d) and the reported water-table elevations from Adams et al. (1964) and Boggess et al. (1964) found maximum water-table elevations at two observation wells (1472 and 1482) less than 0.3 m below land surface, and 0.6 m above land surface at well 1495 (Fig. 16, Table 8). Linear regression of depth to water table on land-surface elevations was also used to identify locations and magnitudes of possible errors in the water-table elevation data of Adams et al. (1964) and Boggess et al. (1964). Comparison of water-table depth data to the regression equation below shows observed water-table elevation exceeded the predicted value by 1.6 m at well 1495, 0.4 m at well 1472, and 0.77 m at well 1463 (Fig. 16, Table 8).

$$\text{Water-table depth} = 0.512 * (\text{land-surface elevation}) + 0.1612;\quad r^2 = 0.52$$

The observed water-table elevation was less than the predicted value by 0.4 m at well 1482. Thus for the purpose of computing RMS, the water-table elevations for these wells were adjusted as shown in Table 8. In addition, the water-table elevation for well 1463, located within a large cell near the western edge of the model, was set to the average water-table elevation of the cell. Also, observation wells located within larger constant head, drain, or river cells near the edges of the grid were not included in the calibration data set (not included in Table 8).

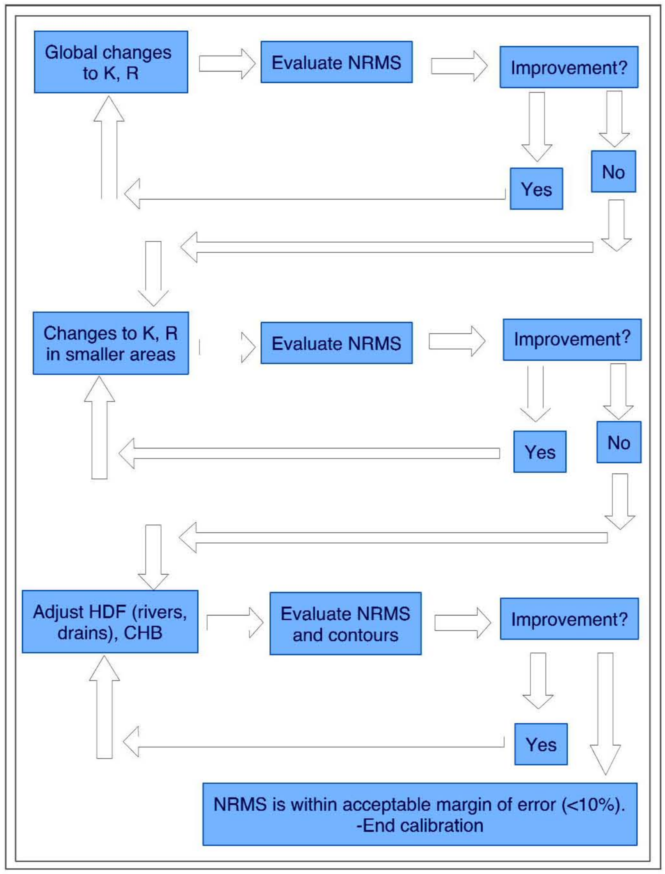

Figure 15. Flow chart for calibration process. (HDF-Head Dependant Flux; CHB-Constant Head Boundary)

Adjustments to the model grid were done to avoid software execution errors and model convergence problems. For example, several constant head boundary cells with head values below the cell bottom of layer 1 prevented the model from running. In other areas, because the elevation of the base of layer 1 was close to the elevation of the water table, the rewetting algorithm in the software caused the model to be unable to converge. The solution used to avoid both of these problems was to reduce the elevation of the bases of a small number of cells in layer 1 to values 1 to 2 m less than the water-table elevation from Adams et al. (1964) and Boggess et al. (1964).

Additional drain cells were added to small areas east of Route 1 that are topographically low and contiguous to several small streams but are not depicted as hydrographic features on topographic maps. These drain cells improved the visual fit of the predicted and observed 3-m water-table elevation contours.

Particle Tracking and Wellhead Protection Area Delineation

The Delaware Source Water Protection Assessment Plan (DNREC, 1999) and Wellhead Protection Plan (DNREC, 1990) guidelines state that WHPA delineations completed by modeling should include areas in which water at the water table will travel to the well intake (well screen) in a period of 5 years or less. A process known as particle tracking modeled the 5-year time-of-travel (TOT) area. Particle tracking in Visual MODFLOW is done by MOD-

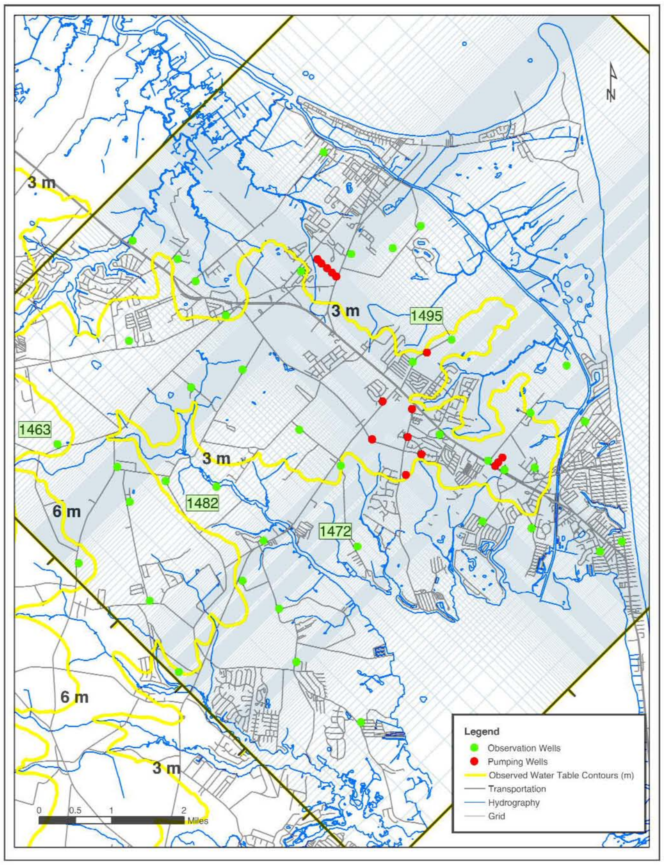

Figure 16. Water-table elevations and observation well locations from 1964 USGS Hydrologic Atlas Series maps by Adams et al. (1964) and Boggess et al. (1964).

Table 8. Observation well identifier, locations, and average ground-water elevation. Water level data from 1964 USGS Hydrologic Atlas Series maps. See text for explanations of head categories.

Well ID	Easting (m)	Northing (m)	Original Head (m)	Modified Head (m)
1333	482476	4290270	1.52	
1334	483474	4289861	2.74	
1336	483875	4289370	1.22	
1337	486721	4292239	2.13	
1338	486217	4289589	4.88	
1339	487331	4289974	1.83	
1340	488875	4290599	1.22	
1341	488258	4290106	1.52	
1463	480807	4285753	**6.71**	5.94
1467	481281	4283106	6.40	
1468	482411	4284470	4.27	
1469	482856	4282268	4.57	
1470	484921	4282713	2.44	
1471	485383	4283606	1.83	
1472	487472	4283475	**2.13**	1.72
1473	487100	4285273	3.05	
1474	489297	4285968	3.66	
1475	488696	4287578	3.96	
1476	484550	4288611	2.74	
1477	484918	4287407	3.96	
1478	483776	4287013	3.96	
1479	486180	4286069	4.27	
1480	482396	4288045	3.96	
1481	483207	4284930	2.44	
1482	484338	4284803	**0.61**	0.94
1483	483504	4280689	3.05	
1487	487548	4279573	0.61	
1488	486116	4280912	1.52	
1495	489563	4288072	**4.27**	2.66
1496	492121	4287498	1.52	
1498	492527	4286251	2.74	
1499	493344	4283590	1.83	
1500	492861	4283365	1.22	
1501	491340	4283883	2.44	
1502	490251	4284033	1.83	
1503	490738	4285179	4.27	
1504	491411	4285232	4.88	
1505	491313	4286448	3.05	
Oi24-04	490373	4285384	3.70	
Oi41-01	485731	4282093	2.40	
Oh33-03	482138	4285245	4.40	

PATH (Pollock, 1989), a program that calculates time and direction of travel of particles, on the basis of flow velocity computed from a ground-water pressure field generated by a MODFLOW simulation. MODPATH does not consider effects which may cause the particles to move faster than by advection, such as diffusion or dispersion (Wilson and Achmad, 1995). MODPATH calculates particle tracks both forward and backward in time.

Both forward and backward particle tracking were used in this study. Backward tracking was used to compute particle tracks from wells to where the particles entered the aquifer. In this case, an array of particles was placed in a 10-m radius circle centered on the well and in the layers corresponding to the well screens. Additional tests were run using different shaped arrays of particles (See Pumping and Drawdown). Forward tracking was used to track particles from any location in the model to their eventual discharge at a boundary. In this case, arrays of particles were placed on the perimeter of variably sized circles centered on the wells.

Sensitivity Analysis

Sensitivity analysis is done to evaluate how uncertainties in K and R estimates, discretization of the subsurface into a grid, and configuration of boundary conditions affect the calibrated model and model predictions (Anderson and Woessner, 1992). In this study, the measures of sensitivity are the root-mean-squared error between the predicted water-table elevations and data from Adams et al. (1964) and Boggess et al. (1964) and the sizes of the WHPAs. Sensitivity analysis included several parameters:

1. Evaluating model response to variations of K and R.
2. Evaluating model response to increased vertical resolution, in this case, splitting layer 3 in half.
3. Evaluating model response to addition of an active layer representing the Manokin formation.
4. Evaluating model response to different representations of the ocean boundary.
5. The use of both forward and backward particle tracking for WHPA delineation can be considered a type of sensitivity analysis.

RESULTS AND DISCUSSION

Calibration to Pre-Pumping Conditions

The calibration process in this study consists of trial and error adjustments of input data until simulated heads match observed heads within a predetermined margin of error. The calibration process was considered acceptable when adjustments of variable parameters reduced the NRMS to 8.5 percent, or about 0.5 meters (Fig. 17). Visually, the 3-meter contour of simulated heads from the calibrated model closely matches the 3-meter contour of observed heads (Fig. 18).

In the course of calibration, global changes (increase/decrease) of the K and R index values reduced NRMS from slightly more than 30 percent to slightly less

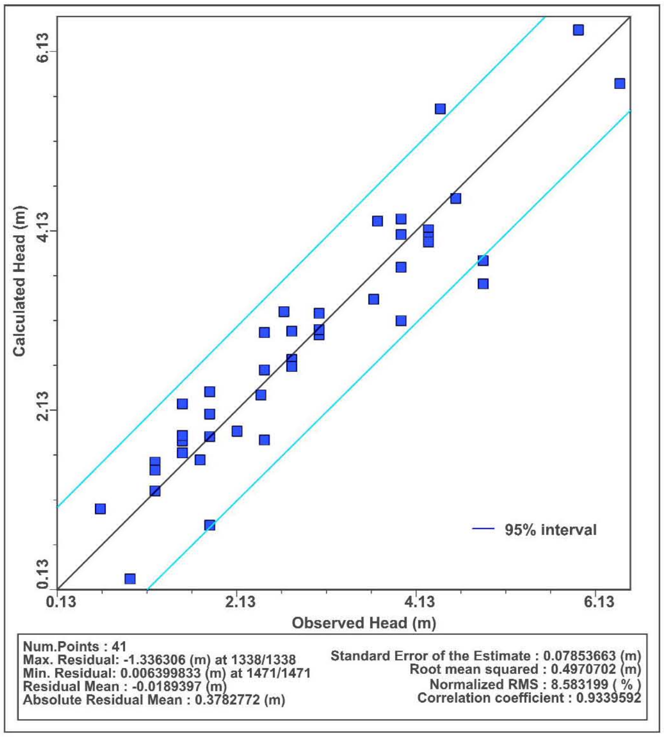

Figure 17. Visual MODFLOW generated plot of observed and calculated water levels at observation well locations. Root mean squared (RMS) and normalized RMS errors shown are within the predefined acceptable range.

than 20 percent. Reduction of NRMS to acceptable levels required changes to values of K and R for specific cells in layer 1 in several areas (Fig. 19). K values were not changed for approximately 69 percent of the area of active cells in layer 1. In comparing the K values from the calibrated model to the original K values derived from the recharge potential maps (Andres, 1991a; Andres and Keyser, 2001; Howard and Andres, 1999), approximately 85 percent of the area of active cells changed less than one recharge potential category (RPC), 8 percent of the area of active cells increased or decreased by 1 RPC, 5 percent of the area of active cells decreased by 2 RPCs, and 1 percent decreased by 3 RPCs. Possible causes for the changes of 2 or more RPCs are erroneous head data in the calibration dataset, errors in K input data (i.e., recharge or resource maps), and improper boundary conditions such as the configuration of the salt-water interface along the Lewes and Rehoboth Canal or the use of constant head boundaries for salt-water marshes.

MODFLOW computes mass balances of water leaving and entering the model to determine if the model satisfies the principle of conservation of mass (MacDonald and Harbaugh, 1988). In the calibrated model, 58 percent of water left the model grid through constant head cells (i.e., ocean, bay, canal, marsh, and Red Mill Pond), and 42 percent left through river and drain cells (i.e., fresh-water streams). Approximately 96 percent of water entered the model grid as recharge, 3 percent entered through constant head cells, and 1 percent through river cells. Almost all of the water entry through river and constant head cells occurred along the cells representing Love Creek and marshes fringing Love Creek. The overall mass balance error of the calibrated model is an acceptable 0.004 percent.

The predicted heads in each model layer are generally similar. Differences between layers reflect variations in boundary conditions and K distributions. The differences in head between the top and bottom layers (Fig. 20) are small over most of the model grid (<0.01 m). Head differences between layers 2 and 4 and 4 and 6 are small over the entire model grid. The largest negative head differences between layer 1 and deeper layers, indicating potential for upward flow, occur in and adjacent to cells located near discharge boundaries representing some marshes and the ocean. The largest positive head differences between layer 1 and deeper layers, which indicate the potential for downward flow, occur in cells located in topographically highest areas (type a, see Fig. 20) of the model grid and in some necks of land surrounded by marsh (type b, see Fig. 20). Model cells of type a are associated with higher K and R values in layers 1 and 2 and indicate areas that likely contribute significant recharge for the entire study area. Model cells of type b are associated with a wide range of K and R values, and, as such, indicate areas of either horizontal flow toward adjacent discharge boundaries or localized vertical flow to deeper model layers.

Pumping and Drawdown

Figure 21 shows the drawdown of the water table predicted by the calibrated model in response to long-term average pumping of the public water wells. For discussion purposes these results are designated baseline expected pumping results. Overall, the volume of water being pumped is roughly 10 percent of the amounts of water entering the model grid as recharge and leaving the model grid through all boundary types.

The greatest drawdown in the vicinity of the Lewes wellfield is approximately 2.5 m and is offset about 55 m from the nearest well (Ni51-29). The offset is due to the interaction of well construction and subsurface heterogeneities. The 1.5-m drawdown contour surrounds all wells in the Lewes wellfield.

A 0.5-m drawdown contour surrounds all wells in the Rehoboth Beach area. Areas of greater drawdown range from 2 m in the eastern section of the wellfield area, to 3.5 m in the western area. The area of maximum drawdown is located approximately 135 m northwest of well Oi22-21.

In this study particle tracking is used to identify land areas where water will infiltrate and travel to pumping wells. Backward particle tracking calculates paths particles would take when moving opposite to ground-water flow, and is a standard method in delineating wellhead protection areas (Wilson and Achmad, 1995; Andreasen and Smith, 1997). Forward particle tracking calculates paths particles take when moving in the direction of ground-water flow. It is used to predict where and how fast water will move from a site under both stressed (pumping) and unstressed conditions.

In this study, one approach to backward particle tracking utilizes circular arrays (diameter of 1 to 10 m) of 16 to 36 particles centered on each pumping well. Two general types of 5-year TOT areas are observed with all combinations of circle diameter and number of particles, but only one type of 5-year TOT area is observed at any particular well. The first type of 5-year TOT (Fig. 22a) includes the wellhead, while the second type (Fig. 22b) does not include the wellhead. The second type of 5-year TOT area is due to the dominance of

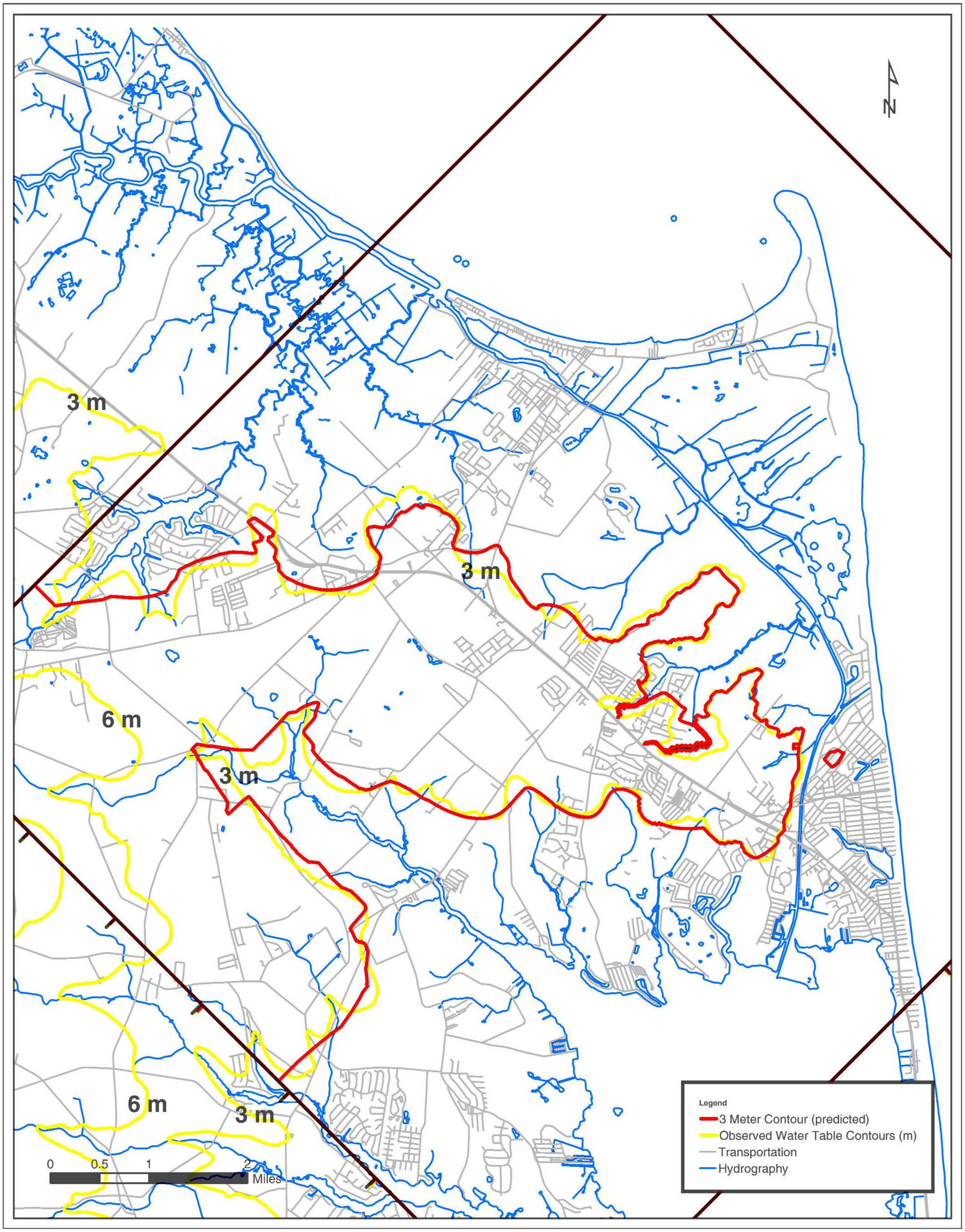

Figure 18. Map showing 3-m water-table contour predicted by the calibrated model and observed water table from Adams et al. (1964) and Boggess et al. (1964). The visual match of the observed and predicted contours is a qualitative tool for evaluating calibration.

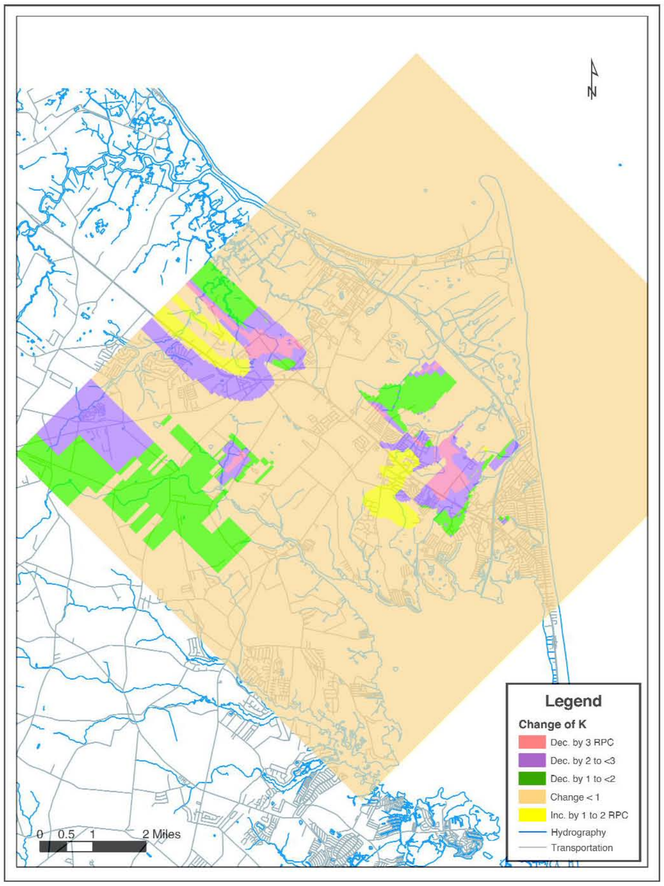

Figure 19. Differences in K in layer 1 between calibrated model and earlier model run. K values were not changed for approximately 85% of the model grid. K changes are depicted in terms of recharge potential categories (RPC). Possible causes for larger changes include errors in the observed head dataset (Adams et al., 1964; Boggess et al., 1964), problems with the recharge potential maps used to generate the starting K distribution, or improper representation of boundaries representing the Lewes and Rehoboth Canal and other salt-water marshes and tidal creeks.

horizontal flow over vertical flow in combination with depths of the well screens and pumping rates. Andreasen and Smith (1997) also report this phenomenon. A second approach, that uses 8 x 5 to 10 x 5 rectangular arrays of particles covering the cells containing pumping wells, also produces two general types of 5-year TOT areas. However, with this approach, the size of the area between the 5-year TOT and the wellhead is smaller than with the first approach. Each approach results in 5-year TOT areas with similar outer perimeters.

A number of simulations were run using forward particle tracking to evaluate if the 5-year TOT areas determined by our implementation of backward particle tracking are adequate to determine WHPAs. In these simulations particles were placed at the water table at different distances from the pumping wells. In some cases the particles were not captured by the pumping wells and moved to down-gradient constant head or drain cells, or more than 5 years elapsed before the particles were captured by the wells. However, some of the particles released in locations between the wellheads and the backward tracking determined 5-year TOT areas were captured within 5 years by the larger wells owned by Lewes and Rehoboth Beach. This indicates that some of the water entering the ground immediately around these wellheads will be captured by the wells. The results provide evidence of the complexity of flow paths in the vicinities of pumping wells and the need for careful assessment of particle-tracking data.

Table 9. Effects of various no-flow boundaries representing saline ground water on NRMS.

Adjustments to boundaries	NRMS %
No adjustments.	8.5
Added constant head cells to layers 2-6.	8.7
Removed all constant head cells from layers 2-5.	8.7
Moved constant head cells to edge of model domain ocean side in layer 6; removed inactive cells.	8.7
Inactive cells represent Delaware Bay and Atlantic, layers 2-4	8.6
Add inactive cells under L&R Canal, layers 2-4	9.2
Add inactive cells under Rehoboth Bay, layers 2-4	9.2

Sensitivity Analysis

Variation of NRMS in response to equal changes of both K and R are relatively minor compared to variation of NRMS in response to changes in one parameter (Fig. 23). This behavior illustrates how a calibrated model is a non-unique solution to actual ground-water conditions. Figure 24 shows an inverse relationship between the areas of 5-year TOT capture zones determined by backward particle tracking and variations in K and R input data. The fact that several models that produce NRMS values in the acceptable range (e.g., NRMS < 10 %) simulate different 5-year TOT areas indicates that results from a single model should not be the sole criterion for determining WHPAs.

Because development usually reduces the amount of recharge, incorporation of land cover data into the recharge input data set is an additional way of testing the sensitivity of the model to variations of recharge data. As expected, reducing recharge also increases the size of the 5-year TOT area.

The position of no-flow boundaries representing saline ground water affects NRMS, but the NRMS values remain under the 10 percent calibration threshold for all of the tested configurations (Table 9). The effects of no-flow boundary locations have little effect on 5-year TOT pathlines (not shown). This indicates that MODFLOW is an appropriate tool for modeling WHPAs in this study and that the calibrated model is not significantly affected by the locations of no-flow boundaries representing saline water. Implementation of no-flow boundaries for cells in layers 2 through 4 under the Lewes and Rehoboth Canal tended to increase the head in cells near the boundary. One problem area for calibration was in this area (Fig. 19), indicating that there may be some locations along the canal where layers 1-4 are saturated with salt water.

The effect of the Manokin formation on modeled ground-water flow in the Columbia aquifer in the Lewes – Rehoboth Beach area was tested by adding an additional active layer to the bottom of the grid and evaluating NRMS and contour patterns resulting from varying the K value of the layer. Recall that in the Lewes – Rehoboth Beach area the top of the Manokin formation is a sequence of silty and clayey confining beds with scattered, more permeable sandy beds (Fig. 3). Modeling the Manokin formation as a single layer relies on the assumption that the hydraulic properties of

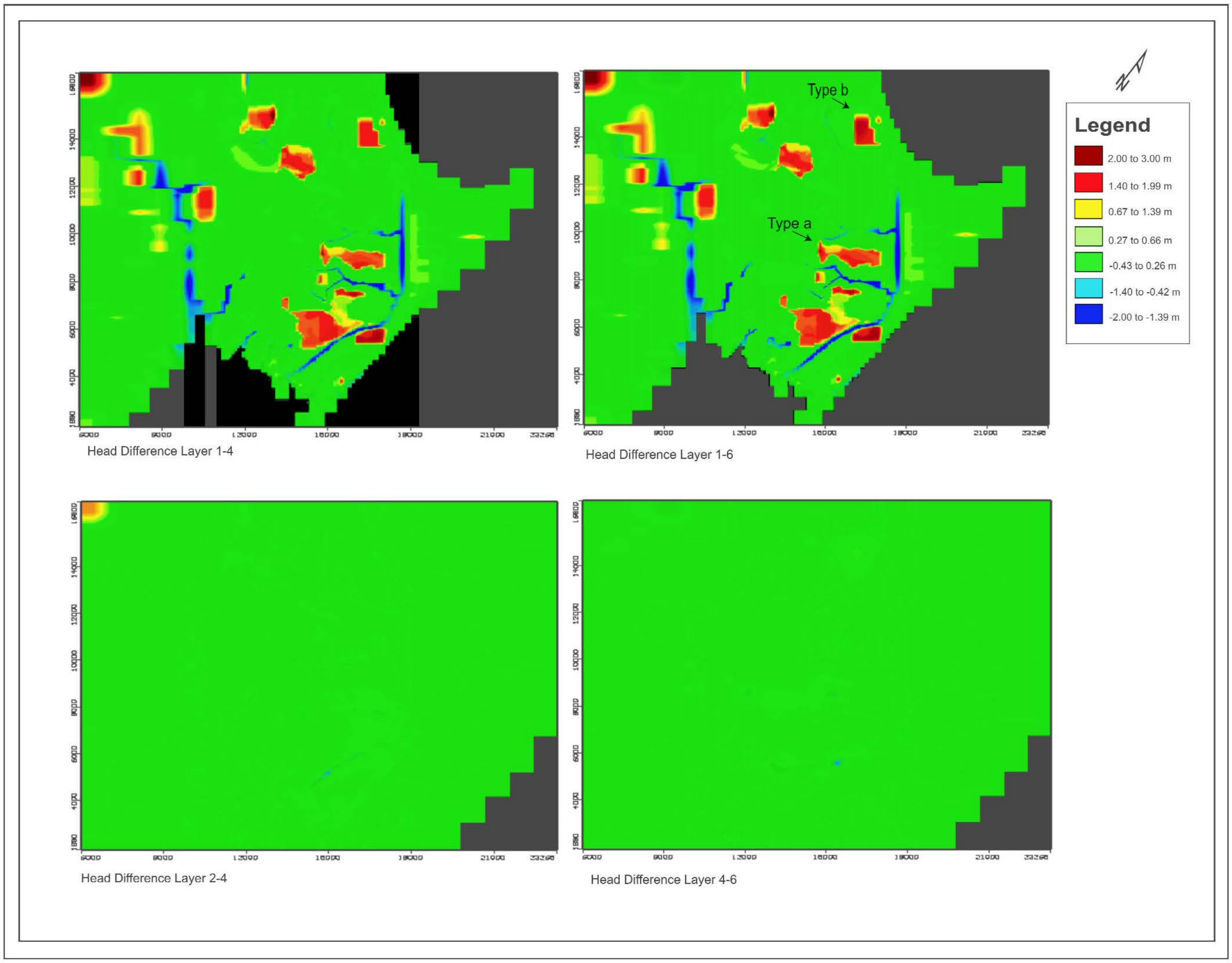

Figure 20. Differences in model predicted heads between layers 1 and 4, 1 and 6, 2 and 4, and 4 and 6. Note the grids are rotated 45º. Type a refers to topographically high areas. Type b refers to areas of land surrounded by marsh.

the confining beds and movement of water through the confining beds have more influence on ground-water flow than flow through the underlying sandy beds. NRMS values exceed the 10 percent calibration threshold at K values equal to and greater than index 9 (0.000096 m/sec) (Fig. 25), values that are in the range of aquifer material. These data indicate that modeling the Manokin formation as an inactive layer does not have a significant effect on this model. This assumption would not be appropriate for a regional scale model that simulates conditions where the top of the Manokin formation does not consist of confining beds. The assumption also would not be appropriate if significant amounts of water were pumped from the Manokin aquifer in the study area in the future.

WHPA Recommendations

WHPA recommendations (Fig. 26) are formulated on the range of 5-year TOT areas from simulations that incorporate uncertainties in aquifer and recharge data (i.e., sensitivity analysis), effects of land cover, and the different types of particle tracking approaches. The recommended WHPAs include a 100-m buffer zone outside of the baseline expected 5-year TOT areas and a buffer zone between the wellheads and the 5-year TOT areas. The buffer zones allow a conservative margin of safety that is designed to provide means to protect the quality of water entering the wells under the full range of expected conditions.

The total area for all WHPAs in the Lewes and Rehoboth Beach areas, including the 100-meter buffers, as determined in this study is 3.69 km^2. The total WHPA encompassing the Lewes wells equals almost 1.39 km^2, 0.93 km^2 in the 5-year TOT areas, and 0.46 km^2 in the 100-m buffer. Those around Tidewater Utilities' wells amount to 0.46 km^2, with 0.08 km^2 in the 5-year TOT areas and 0.38 km^2 in the 100-m buffer. Rehoboth Beach's wells have a total protection area of 1.84 km^2, with 1.02 km^2 in the 5-year TOT areas and 0.82 km^2 in the 100-m buffer.

The WHPAs do not incorporate potential effects of changes in pumping on capture zones. WHPA delineations should be revised when changes to pumping by addition or removal of wells or pumping rate modifications have been completed. The existing model will accommodate pumping rate modifications without significant additional work; however, addition of new wells may require modifications to the grid that in turn would necessitate efforts to adjust boundaries and recalibrate the model.

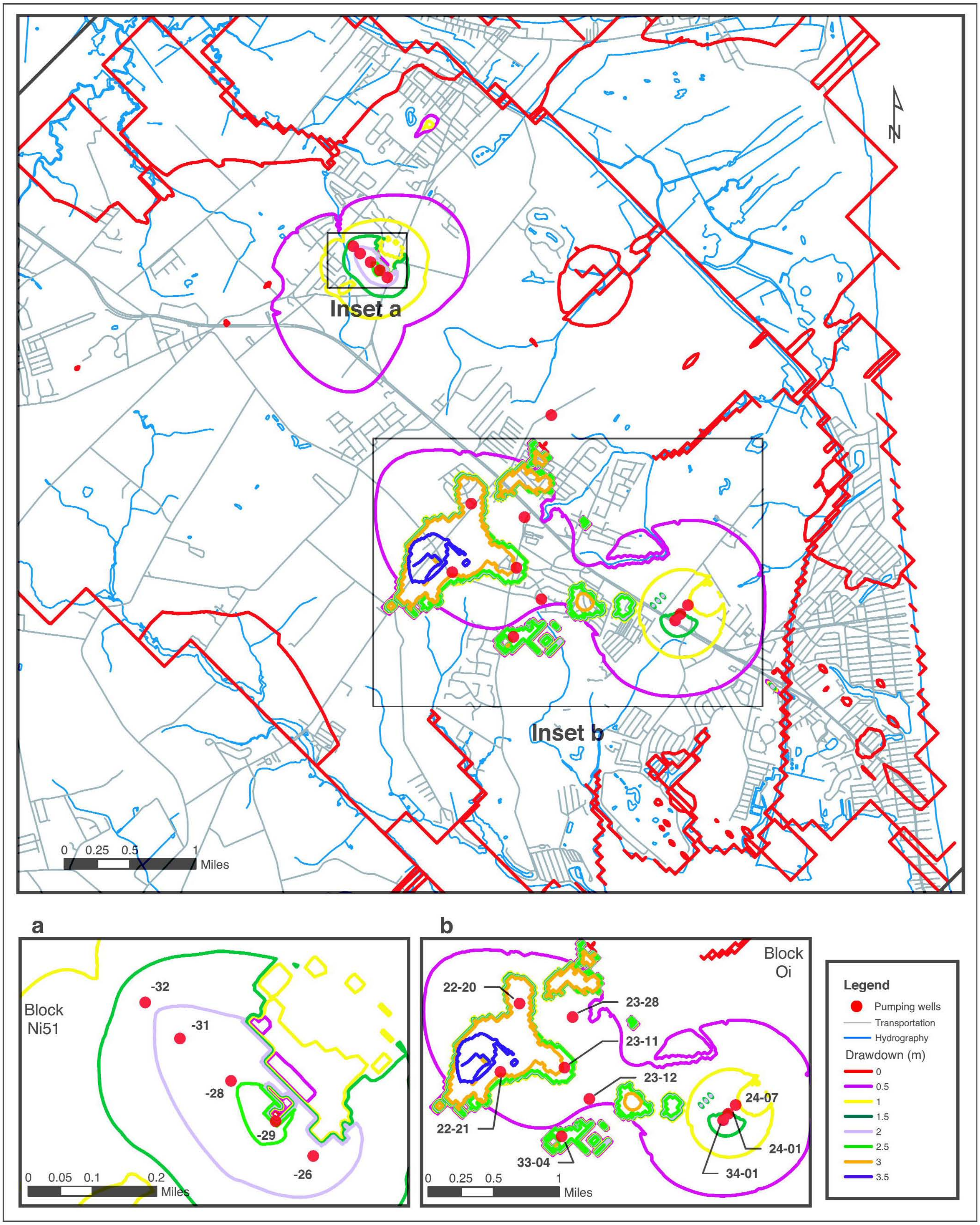

Figure 21. Map of model predicted drawdown. Block Ni51 refers to DGS 1-minute grid identifiers. Block Oi refers to DGS 5-minute grid identifiers.

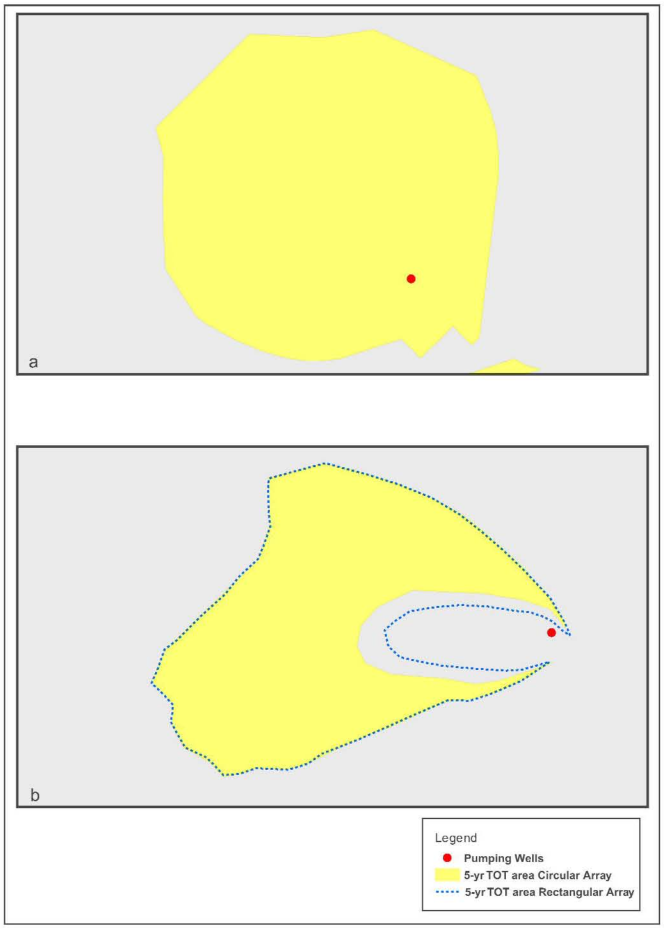

Figure 22. Illustrative example of two types of 5-year time of travel (TOT) areas predicted by model. The 5-year TOT area includes the wellhead in the first type (type a) but does not in the second type (type b). Only one type of TOT area is observed at any one well.

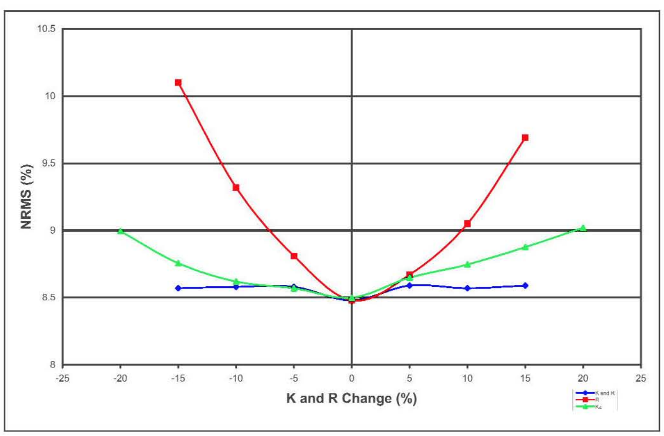

Figure 23. Plot of normalized root mean squared (NRMS) error resulting from changes to K and R. Note that NRMS changes are relatively small when both K and R are changed within the ranges of expected values, but that NRMS changes are much larger when only K is changed. This illustrates that the calibrated model is not a unique solution to solving ground-water flow equations.

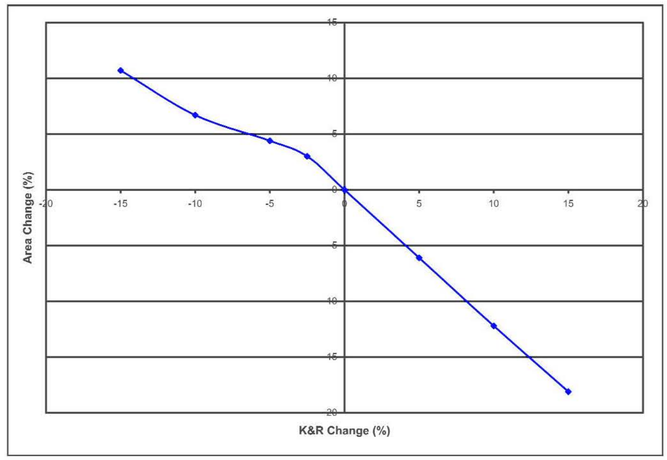

Figure 24. Plot showing sensitivity of model predicted 5-year backward time-of-travel (TOT) capture zone areas to changes of K and R. All of these TOT areas are associated with normalized root mean squared errors of less than 10 percent.

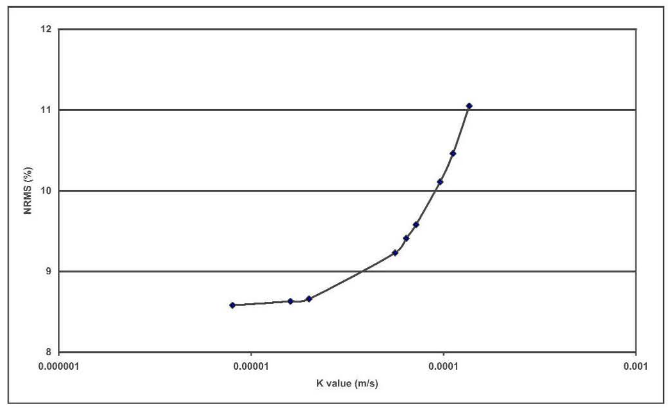

Figure 25. Plot showing sensitivity of NRMS to inclusion of Manokin formation in the model. These data indicate that modeling the Manokin formation as an inactive layer does not have a significant effect on this model. See text for further discussion.

CONCLUSIONS

The results of steady-state, finite-difference, ground-water flow simulations with forward and backward particle tracking were used to identify the 5-year time of travel capture zones and to delineate wellhead protection areas (WHPA) for 15 public water-supply wells in the Lewes-Rehoboth Beach area of Delaware. All wells withdraw water from the Columbia aquifer. In the study area, the Columbia aquifer is heterogeneous and stratified so that it behaves as an unconfined or leaky confined aquifer.

The City of Lewes, the City of Rehoboth Beach, and Tidewater Utilities, Inc. operate the wells included in the study. Because the model was operated under steady state conditions, long-term average pumping rates were used in the model.

The Visual MODFLOW-based model used for delineating WHPAs consists of 263 rows, 200 columns, and 6 layers, with hydraulic conductivity and recharge being simulated as spatially variable. The model represents bodies of sur-

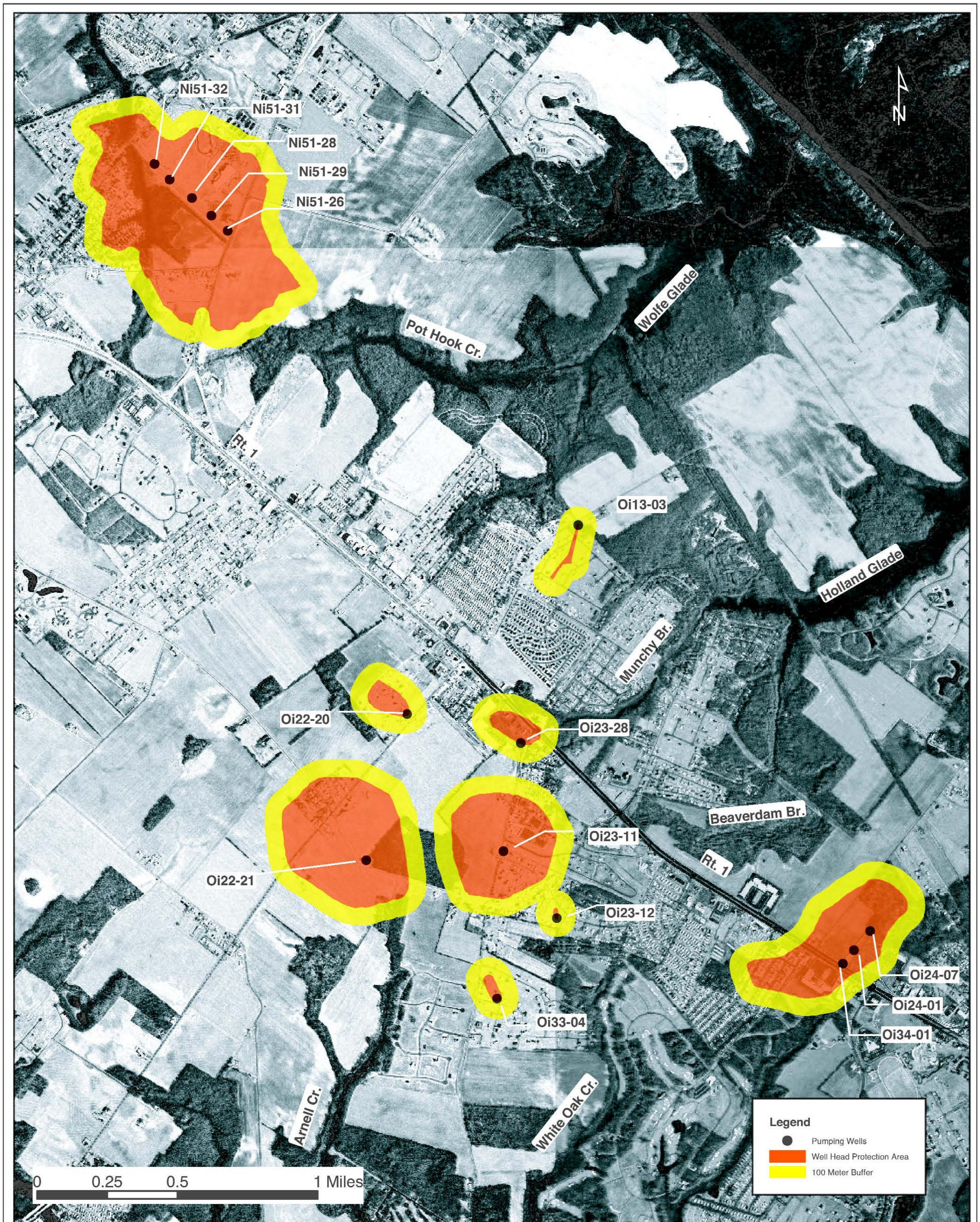

Figure 26. Map showing recommended WHPAs. The WHPAs include 100-m buffer zones around the outside of the 5-year TOT area and, for some wells, a buffer zone between the wellheads and the 5-year TOT area.

face water with river, drain, constant head, and no-flow boundary types. The model was calibrated to water levels observed between 1958 and 1961 in 41 observation wells. A data set containing water levels needed to perform model validation is not available at this time.

The simulation work included analysis of the sensitivity of the model to changes in hydraulic conductivity, recharge, boundary conditions, land cover, number of layers, and initial particle configuration. The recommended WHPAs incorporate the variations in 5-year time of travel capture areas observed in the sensitivity analysis process. As such, the WHPAs are conservative in terms of protecting water quality.

The total area for all WHPAs in the Lewes and Rehoboth Beach areas is 3.69 km^2. The WHPA encompassing the Lewes well field is approximately 1.39 km^2 in size. The size of the WHPA for Tidewater Utilities' wells is 0.46 km^2. Rehoboth Beach's WHPA is 1.84 km^2 in size. The sizes of the WHPAs are representative of current pumping rates and do not include potential effects that would be caused by changing pumping rates.

REFERENCES CITED

Adams, J. K., Boggess, D. K., and Davis, C. F., 1964, Water-table, surface-drainage, and engineering soils map of the Lewes area, Delaware: United States Geological Survey Hydrologic Investigations Atlas HA-103, scale 1:24,000.

Anderson, J. R., Hardy, E. E., Roach, J. T., and Witmer, R. E., 1976, A land use and land cover classification system for use with remote sensor data: United States Geological Survey Professional Paper 964, 28 p.

Anderson, M. P., and Woessner, W. W., 1992, Applied groundwater modeling: San Diego, CA, Academic Press, Inc., 381 p.

Andreasen, D. C., and Smith, B. S., 1997, Hydrogeology and simulation of ground-water flow in the upper Wicomico River basin and estimation of contributing areas of the City of Salisbury well fields, Wicomico County, Maryland: Maryland Geological Survey Report of Investigations No. 65, 87 p, 2 plates.

Andres, A. S., 1986, Geohydrology of the northern coastal area, Delaware Sheet 1, Basic geohydrologic data: Delaware Geological Survey Hydrologic May Series No. 5, scale 1:24,000.

___1987, Geohydrology of the northern coastal area, Delaware-Sheet 2, Geohydrology of the Columbia aquifer: Delaware Geological Survey Hydrologic Map Series No. 5, scale 1:24,000.

___1991a, Ground-water recharge potential map, Fairmount 7.5 minute quadrangle: Delaware Geological Survey, unpublished report and map to the Delaware Department of Natural Resources and Environmental Control, scale 1:24,000.

___1991b, Ground-water recharge potential map, Frankford 7.5 minute quadrangle: Delaware Geological Survey, unpublished report and map to the Delaware Department of Natural Resources and Environmental Control, scale 1:24,000.

___1991c, Methodology for mapping ground-water recharge areas in Delaware's coastal plain: Delaware Geological Survey Open File Report No. 34, 18 p.

___1991d, Ground-water level and chemistry data from the coastal Sussex County, Delaware ground-water quality survey: Delaware Geological Survey Open File Report No. 33, 31 p.

___2003, Ground-water recharge potential, Sussex County, Delaware: Delaware Geological Survey Hydrologic Map Series No. 11, scale 1:24,000.

Andres, A. S., and Brough, B. W., 1994, Ground-water recharge mapping simulation of aquifer contamination under varying recharge potential conditions: Delaware Geological Survey, unpublished report to the Delaware Department of Natural Resources and Environmental Control.

Andres, A. S., and Keyser, T. A., 2001, Ground-water recharge potential map, Rehoboth Beach and Bethany Beach 7.5 minute quadrangles: Delaware Geological Survey, unpublished report and map to the Delaware Department of Natural Resources and Environmental Control, scale 1:24,000.

Andres, A. S., and Ramsey, K. W., 1995, Geologic map of the Seaford area, Delaware: Delaware Geological Survey Geologic Map Series No. 9, scale 1:24,000.

___1996, Geology of the Seaford area, Delaware: Delaware Geological Survey Report of Investigations No. 53, 22 p.

Andres, A. S., and Talley, J. H., 2001, Water use statistics for Lewes water department and Rehoboth Beach water department wellhead protection area delineations: unpublished report to the Delaware Department of Natural Resources and Environmental Control, 6 p. plus Excel spreadsheet.

Bachman, L. J., 1984, Nitrate in the Columbia aquifer, central Delmarva Peninsula, Maryland: United States Geological Survey Water-Resources Investigations Report 84-4322, 51 p.

Bachman, L. J., and Wilson, J. M., 1984, The Columbia aquifer of the Eastern Shore of Maryland: Maryland Geological Survey Report of Investigations No. 40, 144 p.

Benson, R. N., ed., 1990, with contributions by A. S. Andres, R. N. Benson, K. W. Ramsey, and J. H. Talley, Geologic and hydrologic studies of Oligocene-Pleistocene section near Lewes, Delaware: Delaware Geological Survey Report of Investigations No. 48, 34 p.

Boggess, D. K., Adams, J. K., and Davis, C. F., 1964, Water-table, surface-drainage, and engineering soils map of the Rehoboth Beach area, Delaware: United States Geological Survey Hydrologic Investigations Atlas HA-109, scale 1:24,000.

Delaware Department of Natural Resources and Environmental Control, 1990, State of Delaware Wellhead Protection Program Plan: Dover, DE, 40 p.

Delaware Department of Natural Resources and Environmental Control, 1999, State of Delaware Source Water Assessment Plan: Dover, DE, 302 p.

Freeze, A. R., and Cherry, J. A., 1979, Groundwater: Englewood Cliffs, NJ, Prentice-Hall, Inc., 604 p.

Groot, J. G., and Jordan, R. R., 1999, The Pliocene and Quaternary deposits of Delaware: Palynology, ages, and paleoenvironments: Delaware Geological Survey Report of Investigations No. 58, 41 p.

Groot, J. G., Ramsey, K. W., and Wehmiller, J. F., 1990, Ages of the Bethany, Beaverdam, and Omar formations of southern Delaware: Delaware Geological Survey Report of Investigations No. 47, 19 p.

Hinaman, K. C., and Tenbus, F. J., 2000, Hydrogeology and simulation of ground-water flow at Dover Air Force Base, Delaware: United States Geological Survey Water-Resources Investigations Report 99-4224, 72 p.

Hodges, A. L., 1983, Hydrology of the Manokin, Ocean City, and Pocomoke aquifers of southeastern Delaware: Delaware Geological Survey Report of Investigations No. 38, 60 p.

Howard C. S., and Andres, A. S., 1998, Ground-water recharge potential map, Ellendale, Georgetown, and Milton 7.5 minute quadrangles: unpublished report and maps to the Delaware Department of Natural Resources and Environmental Control, scale 1:24,000.

___1999, Ground-water recharge potential maps, The Lewes and Cape Henlopen 7.5 minute quadrangles: unpublished report and maps to the Delaware Department of Natural Resources and Environmental Control, scale 1:24,000.

Johnston, R. H., 1973, Hydrology of the Columbia (Pleistocene) deposits of Delaware: An appraisal of a regional water-table aquifer: Delaware Geological Survey Bulletin No. 14, 78 p.

___1976, Relation of ground water to surface water in four small basins of the Delaware coastal plain: Delaware Geological Survey Report of Investigations No. 24, 56 p.

___1977, Digital model of the unconfined aquifer in central and southeastern Delaware: Delaware Geological Survey Bulletin No. 15, 47 p.

Jordan, R. R., 1962, Stratigraphy of the sedimentary rocks of Delaware: Delaware Geological Survey Bulletin No. 9, 51 p.

___1964, Columbia (Pleistocene) deposits of Delaware: Delaware Geological Survey Bulletin No. 12, 69 p.

MacDonald, M. G., and Harbaugh, A. W., 1988, A modular three-dimensional finite-difference ground-water-flow model: United States Geological Survey Techniques of Water-Resources Investigations, Book 6, Chap. A1, 586 p.

Owens, J. P., and Denny, C. S., 1979, Upper Cenozoic deposits of the central Delmarva Peninsula, Maryland and Delaware: United States Geological Survey Professional Paper 1067-A, 28 p.

Pollock, D. W., 1989, Documentation of computer programs to compute and display pathlines using results from the U.S. Geological Survey modular three-dimensional finite-difference ground-water flow model: United States Geological Survey Open-File Report 89-381, 188 p.

Ramsey, K. W., 1993, Geology of the Milford and Mispillion River quadrangles: Delaware Geological Survey Geologic Map Series No. 8, scale 1:24,000.

___1997, Geology of the Milford and Mispillion River quadrangles: Delaware Geological Survey Report of Investigations No. 55, 40 p.

___1999, Cross section of Pliocene and Quaternary deposits along the Atlantic coast of Delaware: Delaware Geological Survey Miscellaneous Map No. 6.

___2001, Geologic map of the Ellendale and Milton quadrangles, Delaware: Delaware Geological Survey Geologic Map Series No. 11, scale 1:24,000.

___2003, Geologic map of the Lewes and Cape Henlopen quadrangles, Delaware: Delaware Geological Survey Geologic Map Series No. 12, scale 1:24,000.

Ramsey, K. W., and Schenck, W. S., 1990, Geologic map of southern Delaware: Delaware Geological Survey Open File Report No. 32, scale 1:100,000.

Reilly, T. E., 2001, System and boundary conceptualization in ground-water flow simulation: Techniques of Water-Resources Investigations of the United States Geological Survey, Book 3, Chapter B8, 30 p.

Talley, J. H., 1988, Geohydrology of the southern coastal area, Delaware: Delaware Geological Survey Hydrologic Map No. 7, Sheet 2, Geohydrology of the Columbia aquifer, scale 1:24,000.

Talley, J. H., and Andres, A. S., 1987, Basic hydrologic data for coastal Sussex County, Delaware: Delaware Geological Survey Special Publication No. 14, 101 p.

Talley, J. H., and Windish, D. C., 1984, Instructions for preparation of DGS data base schedules: Delaware Geological Survey Special Publication No. 11, 119 p.

United States Geological Survey, 1991a, Lewes quadrangle 7.5 minute series topographic map, scale 1:24,000.

___1991b, Cape Henlopen quadrangle 7.5 minute series topographic map, scale 1:24,000.

___1991c, Fairmount quadrangle 7.5 minute series topographic map, scale 1:24,000.

___1991d, Rehoboth Beach quadrangle 7.5 minute series topographic map, scale 1:24,000.

Waterloo Hydrogeologic Inc., 2002, Visual MODFLOW manual: Waterloo, Ontario, Canada, Waterloo Hydrogeologic Inc., 311 p.

Wilson, J. M., and Achmad, G., 1995, Delineation of wellhead protection areas using particle tracking analysis and hydrogeologic mapping, Northern Anne Arundel County, Maryland: Maryland Geological Survey Report of Investigations No. 61, 121 p.

Appendix

Conversion factors.

Divide	By	To obtain
millimeter (mm)	25.4	inch (in)
meter (m)	.03048	foot (ft)
kilometer (km)	1.609	mile (mi)
square kilometer (km^2)	2.59	square mile (mi^2)